UNIVERSIDADE FEDERAL DO RIO DE JANEIRO
ESCOLA POLITÉCNICA

Departamento de Engenharia Metalúrgica e de Materiais

UFRJ

EVALUATION OF da/dN vs ΔK CURVES AND FATIGUE THRESHOLD VALUES (ΔK_{th}) OF API-X65 STEEL FOR PIPELINES

Author: Daoud Marouan Lmtiui

Tutor: Enrique Mariano Castrodeza

JULY 2016

« Je suis de ceux qui pensent que la science est d'une grande beauté. Un scientifique dans son laboratoire est non seulement un technicien: il est aussi un enfant placé devant des phénomènes naturels qui l'impressionnent comme des contes de fées. »

Marie Curie (1867-1934)

ACKNOWLEDGMENTS

To begin with, I would like to thank my parents for allowing and encouraging me to go wherever my curiosity has lead me during these years in university.

To my brother and my sisters, who always have been there to support and to cheer me to continue going forward.

To my tutor, Enrique, for his help and guidance on this work and for his closeness in the academic life and outside of it.

To all members of the Laboratório de Mecânica da Fratura (LAMEF) at Escola Politécnica-UFRJ for welcoming me with open arms as one of them. Specially Joao and Egon, who also helped me infinitely with the fatigue tests.

Finally, to all my friends and every other person that have made this journey to be incredible.

ABSTRACT

The present work addresses the experimental evaluation of fatigue properties of API-X65 steel. Specifically, da/dN vs ΔK curves and fatigue threshold values (ΔK_{th}) are discussed. Using C(T) specimens, Fatigue Crack Growth (FCG) tests were performed at R = 0.1 and R = 0.7 in air and at room temperature, according to E467 ASTM Standard. Data from these tests are then treated and analyzed. For all specimens, da/dN vs ΔK curves are plotted and discussed. MATLAB routines are developed to calculate the da/dN rates using raw data of the FCG test machine (MTS Flex Test 40). Paris Law coefficients are obtained and compared to literature values of similar API steels. A fatigue threshold value was obtained at R = 0.7. The influence of load ratio (R) is also analyzed.

Finally, a comparison and discussion of all the results obtained in this work is done with values found on other studies.

TABLE OF CONTENTS

LIST OF FIGURES

LIST OF TABLES

1. INTRODUCTION

API 5L steels are widely used in pipeline engineering, for onshore and offshore applications. Since their development, starting with API X42 grade, these high strength steels have been improving with time by using different alloy elements or improving the processing methods. This lead to the development of higher grades API steels such as X65, X70 and X80 ones. For API steels, the last numbers indicate their minimum yield strength in ksi. Research is still continuing on these materials, such that more recent grades were developed, as X100 and X120. Higher mechanical properties and lowering the C content, to ensure good weldability and toughness, are the main themes of research as well as the study of fatigue behavior in different environments, such as seawater, in presence of H_2S, etc.

During their operation, pipelines are subjected to pressure differences related to the fluid or gas they are transporting, mechanical stresses caused by external factors, such as platforms movement, and to the influence of its environment (sea, acidic or basic environments, temperature, humidity, etc). As the consequence of these cyclic events, the pipeline could suffer a fatigue process. As in every structural element under a fatigue process, a fatigue crack growth study needs to be performed in order to ensure the structure integrity and estimate the structure's life. In this line, when evaluating fatigue properties of cracked structures, da/dN vs ΔK curves seem to be the best tool. Lots of information are derived from them: fatigue threshold values, coefficients of the Paris Law which is used to estimate the structure's life, influence of load ratio, frequency, environment, etc. Experimental test guidelines for determining fatigue crack growth rates and near-threshold values are presented by E647 ASTM Standard (2011). The standard provides the test procedure and different specimens that can be used, such as the C(T), which is the most often found in the literature. After performing these tests and treating the data, the results obtained should provide a better understanding on the fatigue material behavior and, hence, helping to take the right decisions when facing an engineering application of that material.

1.1 AIMS OF THIS WORK

This work is focused on evaluating da/dN vs ΔK curves and fatigue threshold values of API-X65 steel in air and at room temperature at load ratio R = 0.7. To do so, fatigue crack growth tests were performed on C(T) specimens. Currently in the literature, few studies are done on API steels using high load ratios. Instead, mainly R=0.1 is used. Hence, the comparison of the results here found for R=0.7 is very interesting with those found in other works. Apart from all the fracture mechanics involved, this work was also thought to get to know E647 ASTM Standard and its application to a real case. Furthermore, another aim was to gain knowledge on the fatigue testing machine used for the tests, which was none at the beginning of this work.

1.2 ORGANIZATION

In this chapter, the aims of the work were presented as well as an introduction to contextualize this project.

In chapter two, a little review on fracture mechanics is done, presenting some accidents dealing with fatigue processes. Basic fracture mechanics concepts are then remembered.

In chapter three, API 5L steels are presented.

Chapter four deals with the UOE manufacturing process, which is the one used for pipeline manufacturing.

A summary of E647 ASTM Standard is done is chapter five, which points out the guidelines to be followed in a test for the measurement of fatigue crack growth rates.

In chapter six and seven, the experimental method and the procedure in this work are explained, focusing on the specimens used, the machine setup and the technical procedures used for each of the specimens.

Results of the fatigue crack growth test are found in chapter eight.

Following, in chapter nine, an analysis and discussion of the results is done, as well as a comparison with results in other works.

In chapter ten are summarized the conclusions and recommendations and some suggestions for future works in this line of research.

At the end of this work, appendices are available.

2. FRACTURE MECHANICS

A commonly accepted definition for Fracture Mechanics is that is the engineering field that quantifies the conditions under which a structural element can rupture due to the existence and growth of a dominant crack in the structure.

Fracture mechanics has been developed essentially in XX century from Griffith and Irwin work, which established the fundamentals of elastic fracture mechanics (LEFM) (Anglada, 2002).

Before the development of Fracture Mechanics, structures were designed using only conventional material fail theories, that is, theories based on the plastic collapse of the structure. The presence of small cracks and materials defects was known, but not its role or the effect of variating loading on them (Dowling, 2007).

Fracture Mechanics gained interest in the beginnings of World War II, when a lot of essential war machinery and structures failed in a sudden way, even at stress levels that could not cause problems from the conventional point of view. Many ships and aircrafts failed apparently for no good reason. Later, it was eventually known that these accidents were caused by cracks present in the metallic structures. One of the most known cases, are the Liberty Ships, put on service during World War II. These ships operated in northern seas and experienced brittle fractures. The SS Schenectady, a ship tank corresponding to this series of ships, after 16 days of being c their work quickly for the war. Nevertheless, it was years after that it was known that the main cause was the brittle fracture of low-grade steel components, a problem that was exacerbated by the cold water.

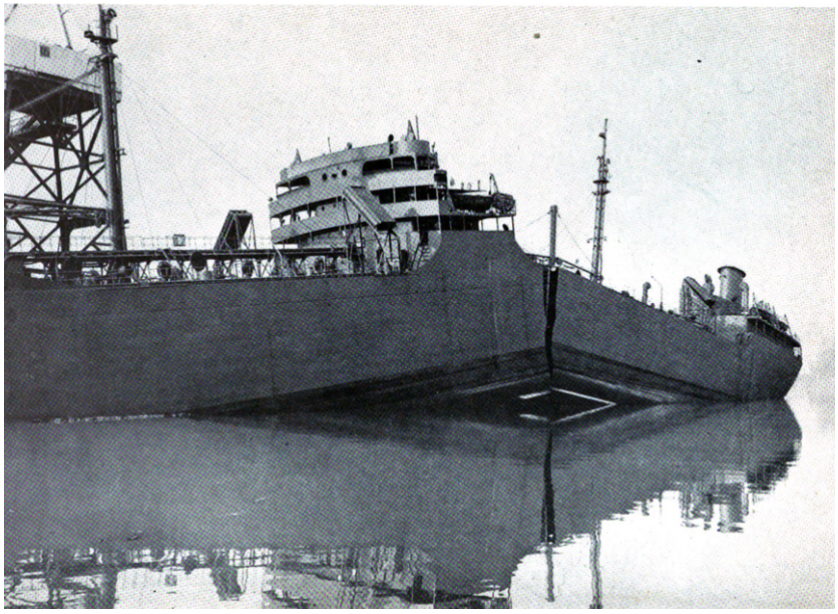

Figure 1. The SS Schenectady after splitting in two in calm water. Source: Wikipedia.

Another well-known case in the aeronautic field is the incidents with the Comet airplanes. Three of them crushed during 1953 and 1954 due to cracks growing from the corners of the square fuselage windows (Fracturemechanics.org).

In the pipeline field, many accidents can also be found due to the existence and growth of cracks in the structure. For instance, on October 27th, 2004, an 8-inch-diameter pipeline transporting anhydrous ammonia ruptured in Kansas, leading to a leak of 772 m^3 of this gas in a creek killing more than 25.000 fish (Figure 2). The economic impact, including the damage and clean-up cost was USD 680.715$.

*The pipe segment that ruptured was removed and sent to the Safety Board's Materials Laboratory for examination and testing. The segment had four external gouges. The approximately 11.7-inch-long rupture occurred at one of the gouges (*Figure 2*). Over most of the rupture length, the gouge penetrated 0.019 inch (approximately 12.2 percent of the pipe wall thickness) into the pipe wall. Within the gouge, shear cracks penetrated the metal. From the base of the shear crack that led to the rupture, a fatigue crack propagated toward the interior of the pipe. The fatigue crack extended approximately 0.080 inch below the shear crack with no external corrosion that resulted in a loss of material thickness* (N.T. Board, 2004).

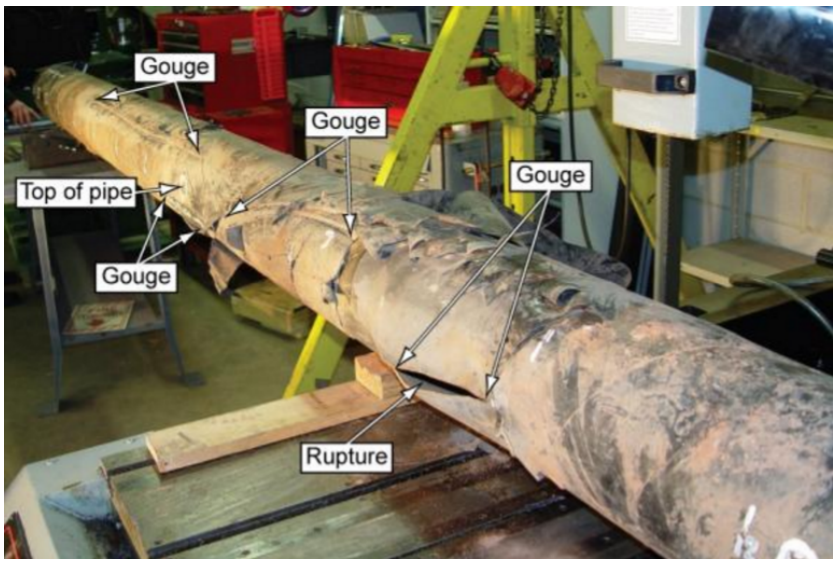

Figure 2. Cracked pipeline and its different zones of interest.

In general, the Fracture Mechanics approach can be divided in two: Linear Elastic Fracture Mechanics (LEFM), which works really well for brittle materials, and Elastic-Plastic Fracture Mechanics (EPFM), which is used in materials that show nonlinear elastic-plastic behavior. Nevertheless, LEFM approach can be used for most materials when they work in fatigue when some conditions are fulfilled. So, the interest and importance of Fracture mechanics is at the top since its study allows engineers to design in a safer manner.

2.1. STRESS CONCENTRATORS

As its name suggests, a stress concentrator, is a region of a piece where stress concentration due to the presence of a geometric discontinuity (a hole, a crack, etc).

Taking into consideration two plane plates, with and without a hole, the lines of force surround the discontinuity creating a new distribution, creating a concentration of lines of force (Figure 3). Hence, the stress that the surrounding zone to the discontinuity is much higher than the nominal stress applied to the plate.

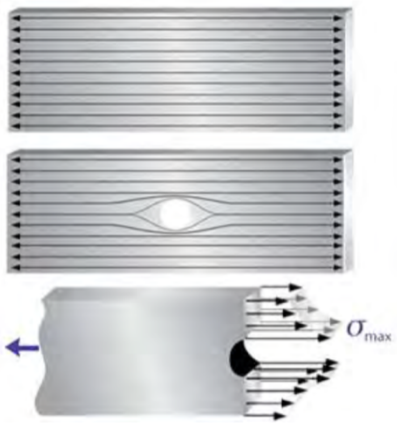

Figure 3. Didactic representation of distribution of lines of force in a plate caused by a stress concentrator. Source: NDT Resource Center (2011).

Inglis studied the stress concentrator state in a plane plate with an elliptical hole in 1913, as shown in Figure 4.

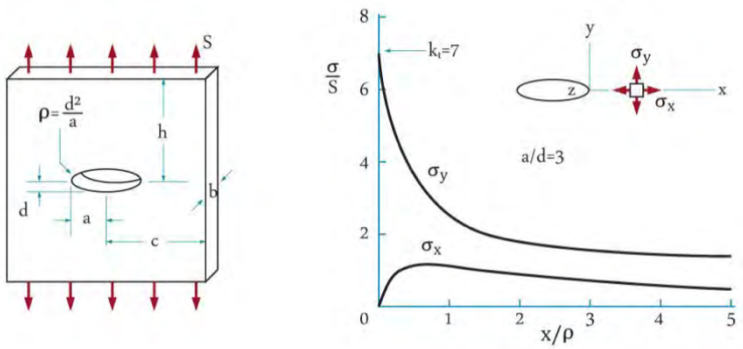

Figure 4. Stress concentrator factor in a plane plate with an elliptical hole (Dowling, 2007).

The stress concentrator factor, k_t, is a ratio between the stress surrounding the discontinuity and the nominal stress applied in the plate, S. Being σ_y the normal stress, k_t is written as $k_t = \sigma_y/S$, where:

$$\sigma_y = S(1 + 2\frac{c}{d}) = S(1 + 2\sqrt{\frac{c}{\rho}}) \qquad (I)$$

Geometric dimensions *c, d* and ρ, are represented in Figure 4, being *ρ* the ellipse radius. Note that in the previous equation, when diminishing *ρ* the higher the value of σ_y is. Then, for a crack, which could be considered to be as an ellipse with an infinite small radius, an infinite value of σ_y should be expected in front of the crack. However, this is not the case, since in metallic materials plastic deformation occurs in close regions to the crack when stress is sufficiently high, as shown in Figure 5 (Dowling, 2007).

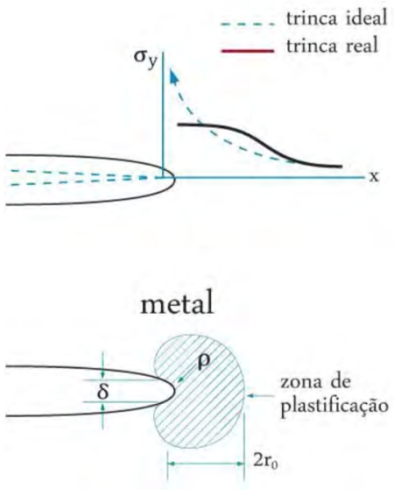

Figure 5. Plastic deformation in front of the crack tip (Dowling, 2007).

2.2. CRACK OPENING MODES

A cracked material can be loaded in three different modes that may act individually or combined. Figure 6 shows represents these three modes. Mode I, also called opening mode, refers to a displacement of the crack surfaces under the action of normal loading. In mode II, shearing mode, the displacement of the crack lips occurs because of shearing loads perpendicular to the crack front. Mode III, tearing mode, is produced by sliding and shearing displacement of the crack lips, in a parallel direction to the crack front. For each mode of loading there is an intensity stress factor, *KI, KII* and *KIII*, associated. In engineering problems, most of the cracks propagate in the opening mode, so the majority of the fracture analyses assume that mode.

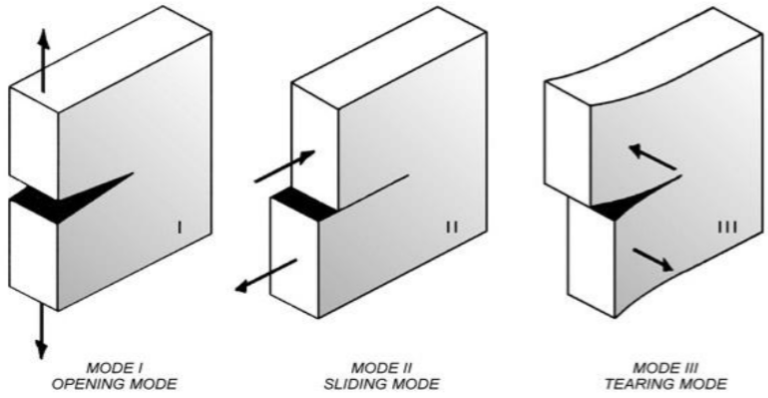

Figure 6. Crack opening modes.

2.3. STRESS INTENSITY FACTOR

Stress intensity factor, *K*, refers to the existent stress magnitudes in front of the crack tip for an isotropic and linear elastic material. It is a theoretical concept that provides a good failure criterion for brittle materials. It is very useful as well for fatigue crack growth problems involving metallic materials.

Stress intensity factors, *K*, are written in the form:

$$K = f(\frac{a}{W})\sigma\sqrt{\pi a} \qquad \text{(II)}$$

Where *a* is the half-crack length, σ is the stress value, and *f(a/W)* is a geometric factor that depends on the geometry and the crack length.

2.4. HIGH CYCLE FATIGUE CRACK GROWTH (FCG)

Failure of a structure may occur even if loaded with lower values of its mechanical resistance when this load is cyclic. Hence, to ensure the structure life and its safety use, this phenomenon has to be well studied.

A mechanism for fatigue crack growth is shown in Figure 7, where plastic deformation

at the crack-tip occurs at low stresses because of defects and local geometry. During the loading and unloading cycle, the crack tip gets a sharper shape that locally increases the stress concentrator. This occurs cyclically causing the crack to grow a *Δa*. The stress field in the crack tip is related to the stress intensity factor, *K*. So for a growth *Δa* of the crack, a ΔK can be associated.

If the maximum applied stress during the cycle is far from the yield strength of the material, there will be small scale yielding at the crack-tip and the Linear Elastic Fracture Mechanics can be applied. In this case the number of cycles required for a complete fracture of the specimen or structure will be high (typically more than 10,000) and the failure mechanism is known as High Cycle Fatigue.

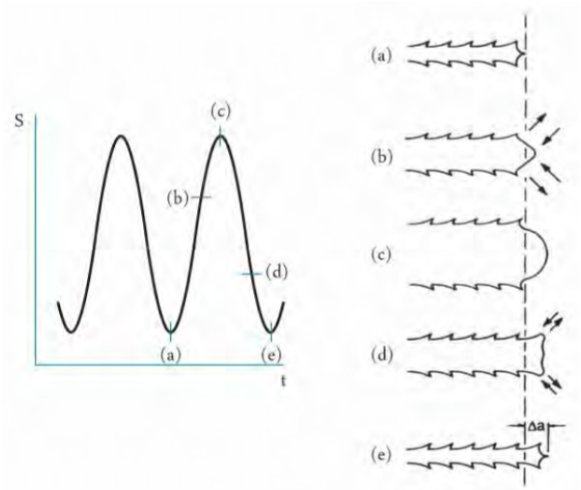

Figure 7. Mechanism of fatigue crack propagation (Dowling, 2007).

Experimentally, fatigue crack growths a little *Δa* for every cycle, and this *Δa* is bigger as higher is the load amplitude. Hence, the fatigue crack growth can be defined as a function of ΔK:

$$\frac{da}{dN} = f(\Delta K) \qquad \text{(III)}$$

Note that no geometry variables are involved in this equation. This is because they

are implicit in ΔK, which already takes them into account in its expression (Dowling, 2007).

The general behavior of fatigue crack growth in metallic materials can be described by the curve in Figure 8, which shows the variation of *da/dN* against *ΔK*. Actually, FCG depends on other factors as well, such as stress ratio, environment, waveform, and frequency. This sigmoidal curve can be seen as three different regimes, which show different behaviors.

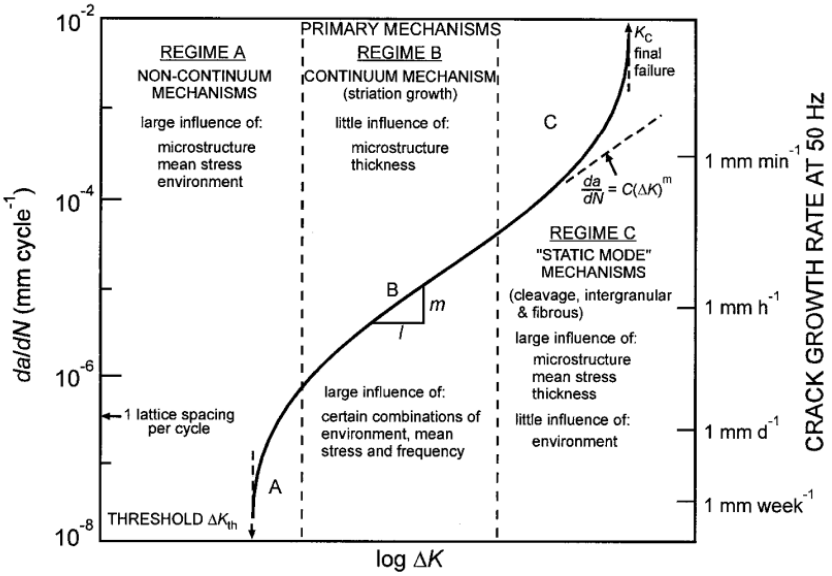

Figure 8. Typical da/dN vs ΔK curve (Ritchie, 1977).

- Regime A

In this regime the crack propagates along the crystalline planes of the material (high shear stress planes at 45º). The plastic zone is so small that it is contained in the grains of the materials, so the crack propagates until it is decelerated by grain boundaries, inclusions or other microstructure barriers (Velázquez, 2004).That is why FCG in this regime is strongly influenced by microstructure and stress level (Totten, 2008).

The threshold is defined in this region. When ΔK is equal or lower to ΔK_{th}, FCG is very slow and it is considered that the propagation has stopped or propagates at non-detectable rates.

The Standard ASTM E647 defines ΔK_{th} as that asymptotic value of ΔK at which da/dN approaches zero. A more empirical description is also given for ΔK_{th} as that ΔK which corresponds to a FCG rate of 10^{-10} m/cycle (E647 ASTM Standard, 2011).

- Regime B

In this stage, there is a linear dependence between log (da/dN) vs log(ΔK), which is described by the Paris Law as follows:

$$\frac{da}{dN} = C(\Delta K)^m \qquad \text{(IV)}$$

Where *C* and *m* are a material property obtained empirically. The constant *m* represents the sensitivity to the load in the crack tip and its value goes, usually, from 2 to 5. Values of *C* and *m* constants of some materials are shown in Table 1.

Table 1. Typical m and C constants given for ΔK in MPa.m$^{0.5}$ and da/dN in m/cycle (J. L. Velázquez, 2004).

Material	m	C x 10^{-11}
Mild steel	3.3	0.24
Structural steel	3.8 – 4.2	0.07 – 0.11
Structural steel in seawater	3.3	1.6
Aluminum alloy	2.6 – 3.9	3 – 19
Copper	3.9	0.34
Titanium	4.4	68.8

When regime II is the dominating part in the fatigue life of the material, the fatigue life can be calculated by integrating the Paris law:

$$Nf = \int_{ao}^{af} \frac{da}{C(\Delta K)^m} \qquad \text{(V)}$$

Although its extended use, the Paris Law is sometimes criticized for not taking into account R, history effects or short-cracks and because it is only valid in LEFM-conditions.

- Regime C

When K_{max} approaches K_{IC}, FGC turns unstable. Now the crack growth is controlled by static modes of failure and there is a strong influence of microstructure, stress level and stress state (plane stress or plane stress loading) (Totten, 2008). Is in this regime, the final failure occurs, which can be fragile or ductile, depending on the mechanical properties of the material.

2.5. EFFECT OF LOAD RATIO (R) IN FATIGUE CRACK GROWTH

The effect of load ratio on crack growth is shown in ***Figure 9***. As already seen, the curve correlating log (da/dN) and log (ΔK) is a sigmoidal that can be divided in three regions. Regions A and C are the ones attributed to be microstructure sensitive when studying fatigue crack propagation. Is in both these regions where the effect of R is more relevant (Ritchie, 1977).

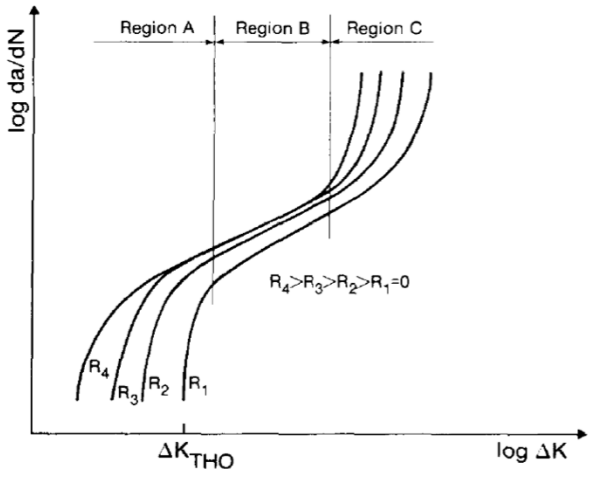

Figure 9. Effect of stress ratio on fatigue crack growth rate (Kujawski, 1987).

In region B, the effect of R is subtler for ductile materials, being more relevant in fragile ones.

Studies working on the influence of R on the near-threshold behavior showed that, in general, for many materials in air ΔK_{th} decreases when R increases. When working in vacuum this trend would be less pronounced.

Klesnil and Lucas proposed a two-parameters empirical relationship between ΔK_{th} and R (Kujawski, 1987):

$$\Delta K_{th} = \Delta K_{th0} (1 - R)^{\Upsilon} \qquad \text{(VI)}$$

Where Υ is a parameter to fit the experimental data, which value would range 0.3 to 1 in air and 0 in vacuum. Another estimation relating ΔK_{th} and R in steels is the one proposed by Dowling, valid for $R \geq 0.1$ (Dowling, 2007):

$$\Delta Kth = 7{,}0\ (1 - 0.85R) \qquad \text{(VII)}$$

To understand the effect of R, crack closure concept was introduced. Briefly, crack closure occurs when crack faces contact before minimum load. So, the effect of this phenomenon would be to reduce crack propagation rate by reduction of the range in stress intensity (Marcus, 1999). Hence, it is necessary to talk about a ΔK_{eff}, defined as:

$$\Delta K = K_{max} - K_{min} \qquad \text{(VIII)}$$

$$\Delta K_{eff} = K_{max} - K_{clos} \qquad \text{(IX)}$$

Where K_{clos} is the crack closure stress intensity factor.

Crack closure phenomenon can occur because of different reasons, including plastic

deformation, surface roughness of the crack, oxidation, etc (Zehnder, 2010).

When R increases the contact of the crack surfaces is less probable. In fact, for R>0.7 it is accepted that the crack surfaces will never touch, even when reaching the minimum value of loading (Zehnder, 2010).

3. API STEELS

Before high strength micro-alloyed steels (HSLA) were developed, steels were strengthened with the addition of C and Mn, which lead to poor weldability and toughness (Soeiro, 2013). As the amount of C in HSLA is low, weldability is good and also keeping good mechanical properties. API steels, starting from X42 grade, are HSLA.

Compared to conventional steels, since HSLA have better mechanical properties, when dimensioning a pipeline, the wall width can be lower, which leads to lower costs of transport and fabrication. Also, if keeping the same wall width, pressure of the liquid or gas transported can be raised; hence production volume transported is increased. Of course, these steels also allow improving the pipeline resistance to environmental conditions such as earthquakes and corrosive environments (Soeiro, 2013).

The API (American Petroleum Institute) specifies the fabrication of pipes through standard 5L, covering seamless and welded steel line pipes. These steels are identified by their yield strength in 1 x 10^3 pound per square inch (ksi). For instance, API steel X65 has as minimum yield strength of 65 ksi (Table 2). For API 5L steels, two levels of product specification are found: PSL 1 and 2. The difference between them is the better or worse fines in some technical requirements such as the equivalent carbon (CE), toughness, yield and ultimate tensile strength, etc.

Table 2. Tensile requirements of some API steels.

	Yield strength (MPa)		Ultimate tensile strength (MPa)	
Steel	Min	Max	Min	Max
X65	448	600	531	758
X70	483	621	565	758
X80	552	690	621	827

API steels are largely used in pipelines. In 1959 in the USA, the first pipeline

completely manufactured using an API steel was built, and the X52 was developed (Malcoln, 2007). During the 60's, this was the most used steel for pipeline construction, with an average content of C of 0.16%. Hence, toughness and weldability wasn't the best ones (Hillenbrand, 1997). At the end of this decade, API steels were produced by high temperature lamination followed by a normalization, which only allowed producing steels until X60 grade. In the beginnings of the 70's, the Thermo Mechanical Controlled Rolling (TMCR) manufacturing process was introduced, which conducted to obtain steels with better mechanical properties and reducing the C content, such as X70 (API 5L Standard, 2004).

In the beginning of the 80's the TMCR processed was improved by cooling down quickly the material after the last stage of the lamination process from 800 to 500ºC. This caused the creation of a bainitic phase, which improved the mechanical properties. This improved process was the Thermo Mechanical Controlled Process (TMCP) (Ordoñez, 2004). Using it, new grades were developed, such as X80. Pipelines were more resistant, so wall thickness could be reduced and, hence, costs as well.

Nowadays, the focus is put on the development of more mechanically resistant API steels, such as X100 and X120 (Corbett, 1988). Another objective is to continue diminishing the C content, to ensure better toughness and weldability.

4. UOE PIPE MANUFACTURING PROCESS

UOE is a method for production of longitudinally welded large diameter pipes that are usually used in onshore and offshore oil and gas pipelines that require high mechanical performance and corrosion resistance (Clennel, 2004). UOE process stands for bending in U, closing in O and later expansion E.

Starting from a large plate, these are formed into circular cylindrical shape through four mechanical steps. The plate edges are first crimped into circular arc. Then the plate is formed into a U-shape using a “U-press”. After this, the plate is pressed into a circular shape in the “O-press” (Figure 10). Afterwards, the seam is welded using submerged arc welding (SAW). To end the process, the pipe is mechanically expanded in order to reach the required final size and to improve its circularity. This last step is critical and greatly important, since low circularity is related to degradation in collapse under external pressure, as may occur when using pipelines in offshore applications (Herynk, 2007).

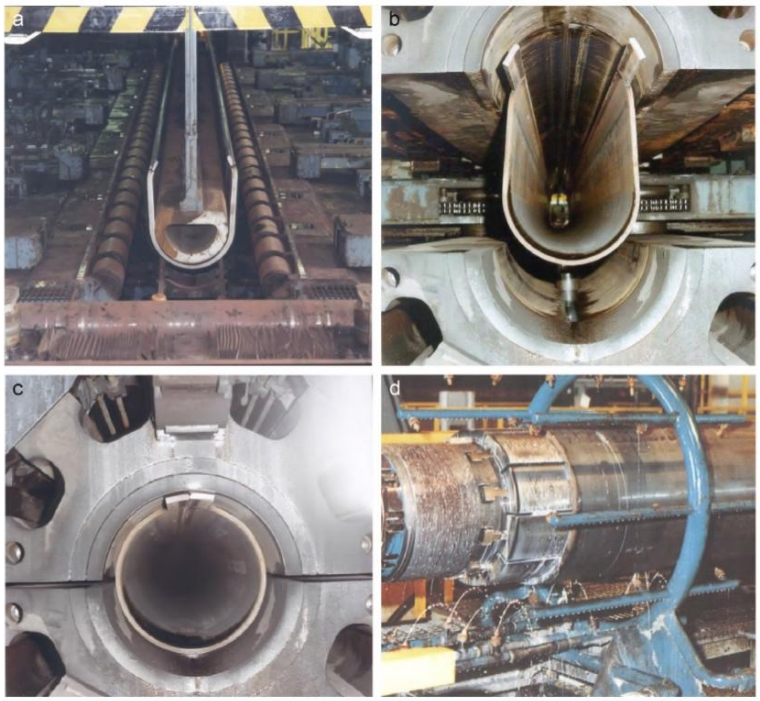

Fig. 3. Photographs of (a) the U-press, (b) and (c) the O-press, and (d) the pipe expander. (Courtesy, Corus Tubes, UK).

Figure 10. UOE process (Courtesy, Corys Tubes, UK).

5. ASTM E647 STANDARD

Procedures covering the determination of fatigue crack growth (da/dN) and fatigue crack growth threshold (ΔK_{th}) are presented in ASTM 647 Standard (Standard test method for measurement of fatigue crack growth rates). Several different test procedures are provided, as well as the details of different specimens that can be used.

5.1. SCOPE

The test consists in applying a cyclic load to a notched specimen, which has been previously pre-cracked in fatigue. Crack length is measured using visually or an equivalent method (optical methods are not recommended since humid environment can difficult the measurements) to obtain the rate of crack growth. Then, this is expressed as function of the stress intensity factor range (ΔK), which is calculated using expressions based on linear elastic stress analysis.

5.2. SPECIMEN GEOMETRY

Three types for specimens are suited for conducting tests according to ASMT 647 Standard, and these are the compact C(T), middle-tension M(T) and the eccentrically-loaded single edge crack tension ESE(T) specimens.

Materials in this method are not limited by thickness or by strength as long as specimens are sufficient thickness to avoid buckling and sufficient planar size to remain predominantly elastic during testing. Another important consideration is that crack closure and residual stress can influence results, although these two variables are not included in the computation of the stress-intensity factor range (ΔK).

In this work the C(T) specimen was used since it is recommended for tension loading, and has the advantage over other types of specimens that requires the least amount of material to study the crack growth behavior. The dimensions of the C(T) recommended by the standard are presented in Figure 11:

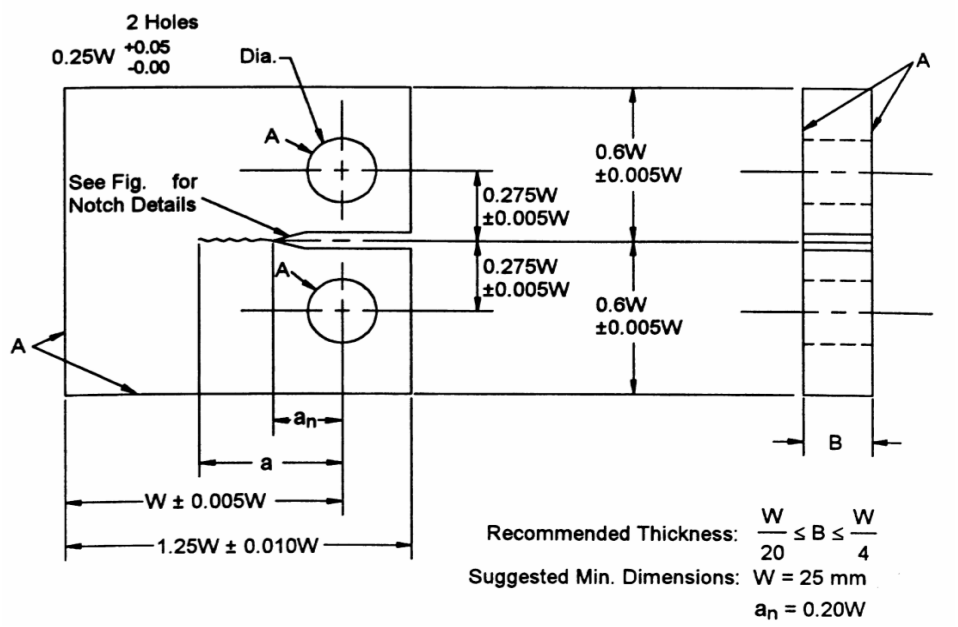

Figure 11. Dimensions for C(T) specimen recommended by E647 Standard.

5.3. NOTCH AND PRECRACK

Notches can be made by several procedures, such as electric discharge machining, milling or saw cutting, depending on the material and the desired precision. Different notch geometries are proposed by the standard (Figure 12). Notch length must be at least 0.2W so that K is not influenced by little variations of location of the two holes where pins are placed.

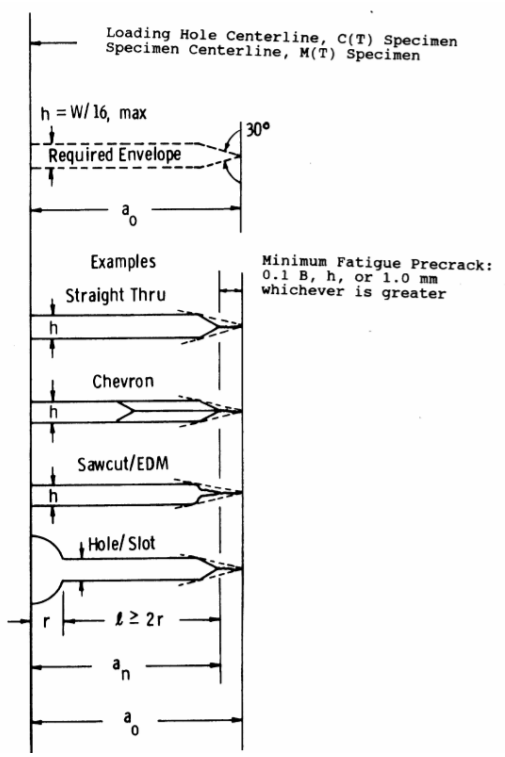

Figure 12. Recommended notches and precrack dimensions.

Precrack must be done in the same conditions as the specimen will be during the fatigue crack growth test. Precracking equipment should be shall be such that the force distribution is symmetrical with respect the machined notch. During precracking, K_{max} should be controlled within ±5%.

The final K_{max} used during precracking cannot be higher than K_{max} to be used in the fatigue crack growth test. Nevertheless, a higher K_{max} can be used to initiate the cracking at the machined notch. In this case, force range shall be stepped down to meet the previous requirement. It is suggested that reductions in the force do not exceed 20% per step and that measurable crack extension occur before proceeding to the next step. Indeed, the force range should be applied in each step over a crack size increment of at least:

$$\left(\frac{3}{\pi}\right)\left(\frac{K'max}{\sigma o}\right)^2 \qquad (X)$$

Where K'_{max} is the terminal value of K_{max} from the previous force step.

Precrack length must be measured in both sides of the specimen with a precision of 0.10mm or 0.002W, whichever is greater. Table 3 presents the maximum and

minimum values of the different variables which the specimen should respect, when working with B = 10 mm.

Table 3. Dimension variables and values defining the geometry of C(T) specimen.

Variable	Symbol	Definition
Width	B	B
Length	W	$\frac{W}{20} < B < \frac{W}{4}$
Base	D	1.25W
Height	H	1.2W
Hole diameter	Ø	0.25W
Crack length before the fatigue	a_n	0.2W
Maximum height of the machine notch	h	W/16
Minimum fatigue precrack	a_{min}	Max {0.1B; h; 1}
Total length of the fatigue precrack	a	$a_n + a_{min}$

5.4. TEST VARIABLES

When working in inert environments or when environmental effects and temperature are not considered, fatigue crack growth can be defined as a function of R and ΔK. And ΔK can be defined as a function of R and K_{max}:

$$\Delta K = (1 - R)\, K_{max} \quad if\ R > 0 \qquad \text{(XI)}$$

$$\Delta K = K_{max} \quad if\ R < 0 \qquad \text{(XII)}$$

Determining da/dN as a function of ΔK allows obtaining results independent from geometry. So, it can be considered that two cracks with different lengths are going to propagate with the same increments per cycle when both of them are under a same ΔK.

To obtain da/dN vs ΔK it is necessary to measure the number of cycles (N) and the crack length (a). To obtain a good distribution of (da/dN, ΔK) points, it is

recommended that data are taken each interval of Δa measured. The standard suggests that these intervals are:

$$\Delta a \leq 0.04W \; for \; 0.25 \leq a/W \leq 0.40 \qquad \text{(XIII)}$$

$$\Delta a \leq 0.02W \; for \; 0.40 \leq a/W \leq 0.60 \qquad \text{(XIV)}$$

$$\Delta a \leq 0.01W \; for \; a/W \geq 0.60 \qquad \text{(XV)}$$

5.5. EXPERIMENTAL METHOD

5.5.1. Constant-Force-Amplitude test procedure for da/dN > 10^{-8} m/cycle

When working with crack growth rates above 10^{-8} m/cycle it is recommended that is specimen is tested at a constant force range (ΔP) and fixed load ratio (R) and frequency.

5.5.2. K-decreasing procedure for da/dN < 10^{-8} m/cycle

This procedure is started by cycling at a ΔK and Kmax level equal to or greater than the terminal precracking values. Then forces are decreased as the crack grows and the test stops when the lowest ΔK or crack growth rate of interest is achieved. If desired, the test may be continued at constant force limits to obtain comparison data under K-increasing conditions. The K-decreasing procedure is not recommended for fatigue crack growth rates above 10^{-8} m/cycle. Force shedding during this procedure must be conducted as decreasing force steps at selected crack size intervals.

The rate of force shedding with increasing crack size must be gradual enough to preclude anomalous data resulting from reductions in the stress intensity factor and concomitant transient growth rates. This is achieved by limiting the normalized K-gradient:

$$C = (\frac{1}{K})(\frac{dK}{da}) > -0.08 \, mm^{-1} \qquad \text{(XVI)}$$

This requirement can be met decreasing the load in steps of 10% every time the crack growths 0.5mm until reaching the minimum value of interest to be measured or when 50000 cycles are done without the crack growing 0.5mm.

5.5.3. Determination of crack length

The crack length is obtained by compliance procedure. Depending on the location of the extensometer, different constants are to be used in the calculus of the crack length using the theoretical expressions given by the Standard (Figure 13).

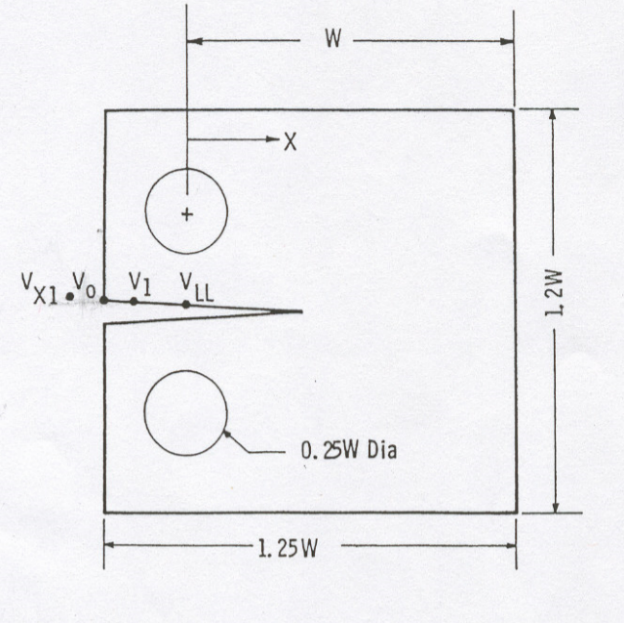

Figure 13. C(T) specimen and specific locations for crack size measurement.

Table 4. Coefficients for theoretical compliance expression.

Meas.	X/W	C_0	C_1	C_2	C_3	C_4	C_5
V_{x1}	-0.345	1.0012	-4.9165	23.057	-323.91	1798.3	-3513.2
V_0	-0.250	1.0010	-4.6695	18.460	-236.82	1214.9	-2143.6
V_1	-0.1576	1.0008	-4.4473	15.400	-180.55	870.92	-1411.3
V_{LL}	0	1.0002	-4.0632	11.242	-106.04	464.33	-650.68

$$\alpha = \frac{a}{W} = C_0 + C_1 u_x + C_2 u_x^2 + C_3 u_x^3 + C_4 u_x^4 + C_5 u_x^5 \qquad \text{(XVII)}$$

$$u_x = \left\{ \left[\frac{EvB}{P} \right]^{\frac{1}{2}} + 1 \right\}^{-1} \qquad \text{(XVIII)}$$

$$0.2 \leq a/W \leq 0.975$$

5.5.4. Determination of stress-intensity factor range ΔK

For the C(T) specimen it is calculated as follows:

$$\Delta K = \frac{\Delta P(2+\alpha)}{B\sqrt{W}(1-\alpha)^{3/2}} (0.886 + 4.64\alpha - 13.32\alpha^2 + 14.72\alpha^3 - 5.6\alpha^4 \qquad \text{(XIX)}$$

$$being\ \alpha = \frac{a}{W} \quad valid\ for\ \frac{a}{W} \geq 0.2$$

Note that in this expression there is the assumption that the material is linear-elastic, isotropic and homogeneous. Also note that possible residual stress effects or crack closure are not computed in this calculation of ΔK.

5.6. VALIDATION CRITERIA

- C(T) specimen must stay in a predominant elastic regime for all the load range values applied. To ensure that:

$$(W - a) \geq \frac{4}{\pi} \left(\frac{Kmax}{\sigma o} \right)^2 \qquad \text{(XX)}$$

- Crack must be symmetric. If the difference of the crack lengths on both sides of the specimen is higher than 0.25B the test in not valid.

- If at any point the crack deviates more than ±20° from the plane of symmetry over a distance of 0.1W or greater, the data are invalid according to this test method.

6. EXPERIMENTAL METHOD

FCG tests for obtaining ΔK_{th} and da/dN vs ΔK curves were performed using C(T) specimens in Laboratory of Fracture Mechanics (LAMEF) at Escola Politecnica -UFRJ. Specimens were done by a workshop using pipeline material. The machine used was a MTS Flex Test 40.

6.1. MATERIALS AND TEST SPECIMENS

C(T) specimens used were dimensioned according to ASTM 647 Standard, as can be seen in Figure 14 and Table 5:

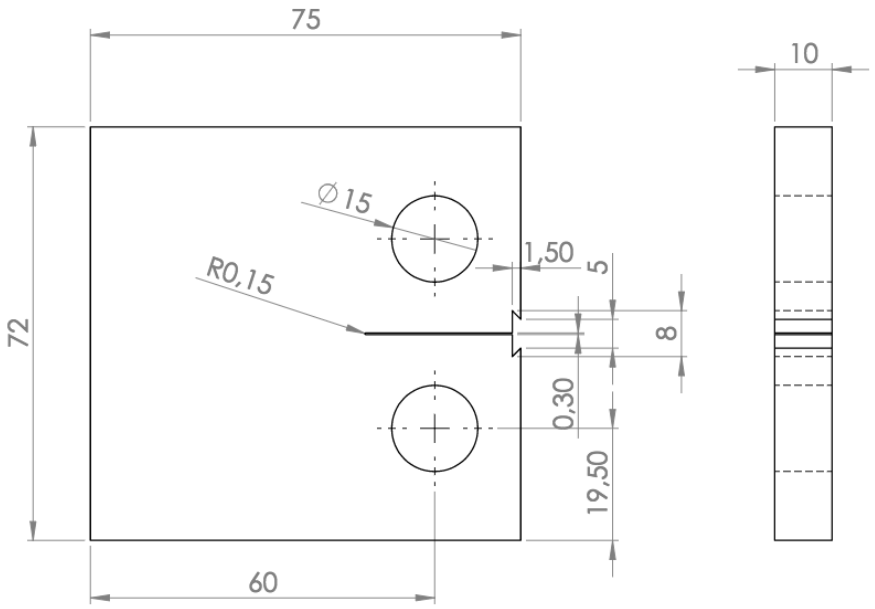

Figure 14. Dimensions of the C(T) specimens used in this work.

C(T) specimens were to be obtained from actual pipelines (Figure 15). In order to optimize the pipeline material available, a SolidWorks model of the pipeline was done where C(T) specimens were placed in the two orientations (Figure 16).

Table 5. Dimensions of C(T) specimen in mm.

B	W	D	h	a_n
10	60	75	0.3	12

Figure 15. Photo of the pipeline from which specimens were obtained.

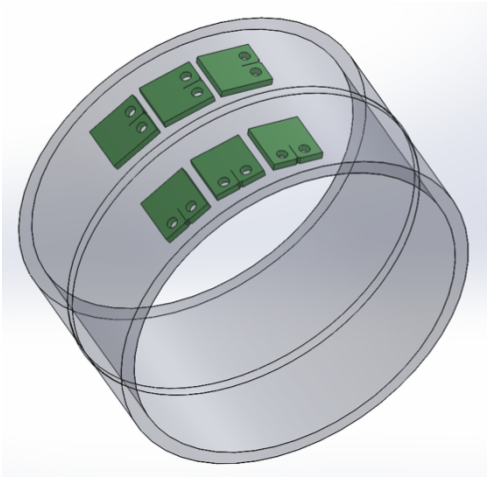

Figure 16. Schematic representation of C(T) specimens in LC and CL orientations.

The material used was an API X65 steel which its mechanical properties in both

orientations are shown in Table 6. Only the base metal material was studied in the LC direction.

Table 6. Mechanical properties of API X65 used in this work.

Property	Orientation	API X65
σ_Y (MPa)	Longitudinal	512
	Transverse	568
σ_R (MPa)	Longitudinal	555
	Transverse	562

To facilitate the crack growth and its observation during the test, C(T) specimens were polished on both lateral sides. Furthermore, polishing also helps to reduce residual stress that may be caused during the specimen manufacturing. The granulometry polishing sheets used were #600.

6.2. MACHINE AND TESTS

A MTS Landmark servohydraulic testing machine was used to perform the tests. Its software can be configured to work with several types of specimens, and it can be programed to work according ASTM E647 Standard. The actuator can be controlled on force or on displacement mode, allowing a large range of configurations to work with.

Two adaptors had to be designed and manufactured since they were not available at the lab, for connecting the force cell and the Clevis. Attention had to be paid to these adaptors since they were also going to be fatigued. To this case, optical inspection in the microscope was performed every certain million number of cycles looking for cracks or any damage in the critical parts of the adaptor.

6.2.1. Number of tests

Three tests were conducted at two different R:

Table 7. Specimens tested.

Specimen	R	Method
CP0	0.1	Constant load
CP1	0.7	Constant load
CP2	0.7	K-decreasing and constant load

6.2.2. Fatigue crack growth length measurement and machine setup

Fatigue crack length was measured throughout the compliance method. A clip was placed in the specimens that registered the COD displacement, which the machine used to calculate the crack length.

Before starting the test, the machine asks to introduce some values, as the specimen dimensions or the constants to be used in the calculation of the crack length (which depend on the position of the clip) and the ones used in delta K calculation.

In the next step, a menu is opened to fill in some test variables, such as the precrack parameters, method of testing, FCG parameters and stop criteria.

7. PROCEDURE

It has to be noted that because the testing machine and its software have been recently installed, in the beginning of this project very little experience on how the FCG software worked was present. This conditioned the time and the procedures.

When starting a new test, the software opened a window where different values should be introduced (Figure 17). Two main groups can be defined: the variables defining the precrack stage and the ones defining the FCG test itself.

Specimens were first precracked a crack length that met the dimensions imposed by the E647 Standard. The variables to be introduced in the software were the final pre crack length, the final K at the end of the precrack stage, the load, the load ratio and frequency. Once the precrack step was done, specimens were ready to start the test. Many variables were to be introduced to define the FCG test, divided in three main parts: FCG parameters, test termination parameters and data storage parameters.

In FCG parameters, the method type is first entered. Two method types are available, the constant load and the K-decreasing method. The first one is used to obtain the da/dN curve, whereas the second one is used to obtain the fatigue crack growth threshold (ΔK_{th}). If the constant load method is chosen, the max load has to be entered in the software (the min load is calculated by the software when R is defined). On the other hand, when choosing K-decreasing method, the initial ΔK at which the test is going to start has to be entered, as well as the normalized K-gradient (C). For both methods, the next variables to be introduced are the frequency at which the FCG test is performed and the type of wave (always a true sine in this work).

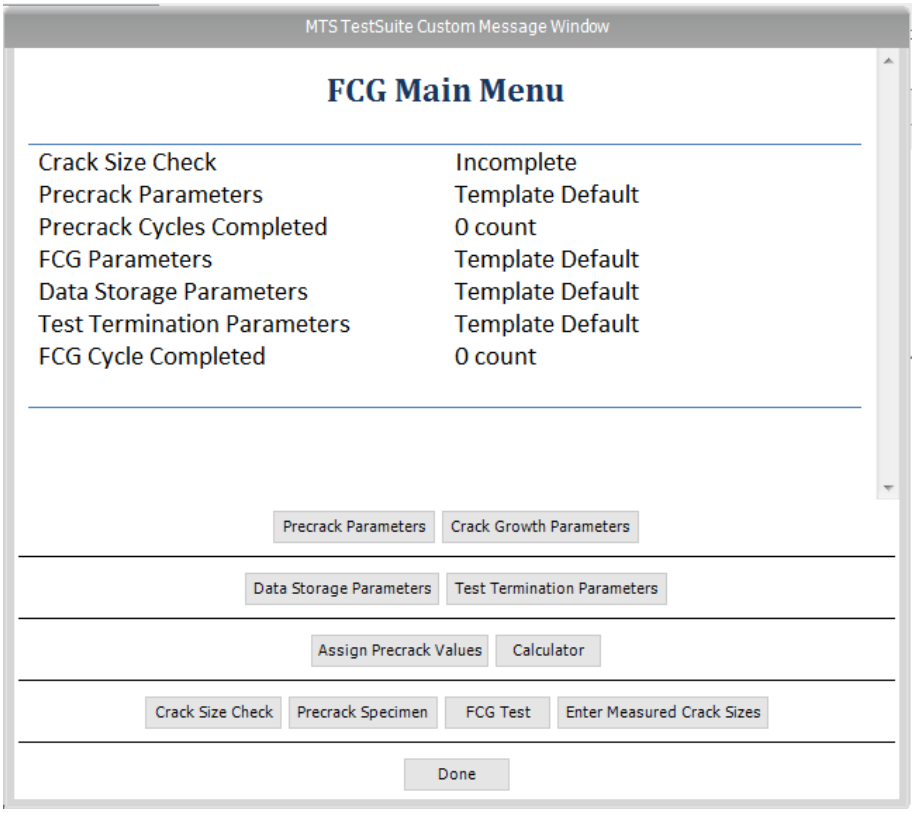

Figure 17. Precrack and FCG parameters menu.

The next group of variables is the Test Termination Parameters. These are conditions that, if reached, stop the test and the machine. In this work, three main conditions were set as limits: a limit crack length, a limit number of cycles and a limit of crack growth rate. Note that the test can also be stopped by decision of the user.

Finally, the Data Storage Parameters, which define how often a data point is recorded by the software. Two conditions were used in this work: a data point would be saved every increase of 0.0006 m in the crack length or every 10000 cycles. At this point, the test can begin.

Once the test was running, three different interlock variables were activated, dealing with the actuator of the machine (displacement and force) and crack tip opening. These were mainly to make the machine stop if the adaptor manufactured broke.

Different values for the FCG test were used for the three specimens, since more was known after every test was performed and the values introduced were more accurate. Specimens CP0 and CP2 were performed in parts (a part is defined here a

stage in which the machine was stopped for any reason), so at the end of each part the values of the previous step had to be introduced as initial values in the software in order to begin the test at the same point where it was stopped. In these cases, where the complete test was performed by parts it was good to use the Crack size check measurement. This option offered also by the software, allowed updating the actual crack size at the beginning of each part. To perform the crack size measurement, the software asked for a maximum load to be applied in this measurement, which would be reduced by a factor (%) also previously introduced. It was really important that the actual load applied did not exceed the load used in the test, in order to not deform plastically the crack tip. In the following, the specific procedure for each specimen is presented.

7.1. CP0: X65TTL R=0.1

Specimen CP0 was available in the lab and had already been precracked by compression. The precrack length was 13 mm. In order to learn how the machine worked, it was decided to use this specimen as an initial test. As the objective in this case was to obtain the da/dN curve, the constant load method was used. The FCG parameters and test termination parameters for CP0 are showed in Table 8.

Table 8. FCG variables value for CP0.

Method	Constant load
Environment	Air, 25°C
R	0.1
ΔP	4500N
$P_{max} - P_{min}$	5000 – 500 N
f	25 Hz
Stop condition	a_f = 0.035 m
	N= 10,000,000
	da/dN = 1 x 10^5 m/cycle

To obtain the da/dN curve of CP0 five parts were needed. As this was the first specimen to be tested, a member of the LAMEF group to make sure no problems arose during the test monitored the machine constantly. So, the machine worked during working hours and labor days. It has also to be noted that the machine was shared and used by different projects, hence the test could not be done in days in a row, depending on the urgency of the other projects. For CP0 the first 4 parts the user stopped the test at the end of the day. Part 5 was ended because the crack size limit was reached (0.035m).

7.2. CP1: X65TTL R=0.7

CP1 was the first specimen precracked in the laboratory. The precrack values introduced in the software were:

Table 9. Precracking variables value for CP1.

Precrack final length (m)	Final ΔK	Load ratio (R)	f	Environment
0.0135	12 ($MPa.m^{0.5}$)	0.1	25	Air, 25°C

Specimen CP1 was also tested using the constant load method to obtain the da/dN curve. The crack limit size condition was increased to be 45mm, against the 42mm in CP0. This was the only test that was done in a row, in one part, without stopping the machine. Since the machine worked really well for CP0 and no problems arose during its functioning, it was decided that the machine could be let on without any member of the LAMEF group monitoring it constantly. Hence, the machine also worked at night. The interlocks (displacement and force of the actuator and COD) were always activated, so if anything “strange” occurred the machine would stop.

Table 10. FCG variables value for CP1.

Method	Constant load
Environment	Air, 25°C
R	0.7
ΔP	4200 N
$P_{max} - P_{min}$	14000 – 9800 N
f	25 Hz
Stop condition	a_f = 0.045 m
	N = 2,500,000
	da/dN = 1 x 10^5 m/cycle

7.3. CP2: X65TTL R=0.7

Specimen CP2 was precracked in the laboratory. The values introduced in the software were:

Table 11. Precracking variables value for CP2.

Precrack final length (m)	Final ΔK	Load ratio (R)	f	Environment
0.0135	12 (MPa.$m^{0.5}$)	0.1	25	Air, 25°C

Specimen CP2 was used to obtain the fatigue crack growth threshold (ΔK_{th}), so the K-decreasing method was used. When using this method and once the lowest value of ΔK or crack growth rate of interest is reached, the E647 Standard allows continuing the test at constant force. So, both ΔK_{th} and the da/dN curve were obtained for CP2. The test was done in 4 parts. The three first parts were to obtain the ΔK_{th} using the K-decreasing method, and the last part was performed at constant load. When the K-decreasing method is chosen, the software asks for the normalized K-gradient (C) and the initial ΔK at which the test will start. Remember that C value is to be greater or equal to -0.08mm^{-1}.

Although the machine was on also during nights, the test was stopped in the K-decreasing method since the machine had to be used for other projects in the laboratory that were urgent. Again, when working in parts and before starting a new one, a crack size measurement was performed to update the crack size in the software and the FCG parameters of the previous part were introduced as the starting ones for the current part.

In the first three parts, the number of cycles at which the machine would stop (test termination parameter - stop condition) was increased when a new part was created. This was because it wasn't first thought that it would take so many cycles to achieve ΔK_{th}. The values of N as stop condition were 3.000.000, 5.000.000 and 10.000.000 for part 1, part 2 and part 3, respectively. The whole K-decreasing part was performed at a frequency of 25Hz except for part 3, which was done at 30Hz, to make the test go faster. However, the machine stopped suddenly when working at 30Hz when N = 8.060.000 cycles. When working at low values of ΔK, the displacement amplitude of the machine actuator is very low, so when working at high frequency, the machine has trouble to achieve those displacement limits at such high speed. This was believed to be the reason to this problem, so it was decided that in the future parts only a maximum frequency of 25 Hz was going to be used during the FCG test.

Table 12. FCG variables value for the K-decreasing method.

Test parts	1, 2 and 3
Method	K-decreasing
Environment	Air, 25°C
C	-0.08 mm^{-1}
ΔK initial	14 $MPa.m^{0.5}$
f	25 - 30
Stop condition	a_f = 0.045 m
	N= 3,000,000 – 10,000,000
	da/dN = 1 x 10^5 m/cycle

Once the K-decreasing stage was done, part 4 was started using the constant load. The values entered in the software were those so that the starting data points of part 4 were those where part 1 started too, in order to obtain a continuous da/dN curve. These values were obtained using the software calculator, which gives the load to be used when wanting to start in a specific ΔK at a specific crack size.

Table 13. FCG variables value for the constant load method.

Test parts	Part 4
Method	Constant load
Environment	Air, 25°C
R	0.7
ΔP	2.100N
$P_{max} - P_{min}$	7.000 – 4.900 N
f	25
Stop condition	a_f = 0.045 m
	N= 6,000,000
	da/dN = 1 x 10^5 m/cycle

7.4. DATA ANALYSIS

Once the test was ended, the machine provided data on the FGC test, such as the final crack size, da/dN, final K max recorded, etc. In order to analyze these data, two procedures were developed in order to compare these values obtained throughout the machine. These two procedures aim to calculate *da/dN* and are the ones recommended in ASTM E647 as data reduction techniques, which are the secant method and the incremental polynomial method.

7.4.1. Secant Method

The secant method, also called point-to-point technique, it is based on the calculation

of the slope of a straight line connecting two adjacent data points on *a* vs *N* curve:

$$\left(\frac{da}{dN}\right)_{\bar{a}} = \frac{a_{i+1}-a_i}{N_{i+1}-N_i} \qquad \text{(XXI)}$$

The da/dN calculated this way is an average rate over a crack lenght increment. Because of that, for the computation of ΔK, the average crack size is used for its calculation: $\bar{a}=1/2(a_{i+1}+a_i)$.

7.4.2. Incremental Polynomial Method

This method is a more sophisticated way to compute da/dN. It involves fitting a second-order polynomial to sets of 2n+1 successive data points, where n is usually 1, 2, 3 or 4. The local fit is described by:

$$\hat{a}_i = b_0 + b_1\left(\frac{N_i-C_1}{C_2}\right) + b_2\left(\frac{N_i-C_1}{C_2}\right)^2 \qquad \text{(XXII)}$$

Where b_0, b_1 and b_2 are the regression parameters that are determined by the least squares method over the range $a_{i-n} \le a \le a_{i+n,}$ and C_1 and C_2 are used to scale the input data:

$$-1 \le \left(\frac{N_i-C_1}{C_2}\right) \le 1 \qquad \text{(XXIII)}$$

The da/dN value calculated at N_i is given by:

$$\left(\frac{da}{dN}\right)_{\hat{a}_i} = \frac{b_i}{C_2} + \frac{2b_2(N_i-C_1)}{{C_2}^2} \qquad \text{(XXIV)}$$

When computing the value of ΔK corresponding to a certain da/dN value, the fitted

crack size $\hat{a}_i$ is to be used.

7.5. ΔK_{th} DETERMINATION

The ASTM 647 Standard defines ΔK_{th} as the ΔK which corresponds to a fatigue crack growth rate of 10^{-10} m/cycle. Using this definition, a minimum of 5 points approximately equally spaced between growth rates from 10^{-9} to 10^{-10} m/cycle were used to calculate a linear regression of log(da/dN) vs log(ΔK). The ΔK_{th} reported is the one corresponding to a da/dN of 10^{-10} m/cycles computed in the calculated linear regression.

8. RESULTS

8.1. TEST SPECIMEN CP0

Data for CP0 were obtained in five parts. The user terminated the first four parts at the end of the day. Table 14 shows the values of some variables at the end of each corresponding part.

Table 14. Variable values at the end of each five parts.

CPO						
PART	Mode	N_f (cycles)	a_f (m)	ΔK (MPa.m$^{0.5}$)	Stop reason	Elapsed time (h)
1	Constant Load	147,500	0.013	8.379	User	1.64
2	Constant Load	599,175	0.015	9.036	User	6.66
3	Constant Load	663,096	0.018	10.253	user	7.37
4	Constant Load	684,458	0.022	12.481	user	7.61
5	Constant Load	709,221	0.035	23.549	Crack size	7.88

Note that for part 1, since the precrack length was 0.013mm, the final crack length (a_f) is also 0.013mm, meaning that the crack length did not grow during the first 147500 cycles. Furthermore, every time the machine started the FCG test, the first data points were not valid since they showed extremely high da/dN values and very dispersed. Maybe, this could be due to the rearrangement of Cottrell atmospheres in the crack tip after the test was interrupted. The first part for CP0 was entirely not valid because of this reason. Note also that the number of cycles at the end of this first part is really low in comparison to a regular FCG test, which makes data not representative. Part 1 was useful in order to know how the variables were introduced, the limits defines, etc. For parts 2 to 5, the crack grew increasing ΔK. The FCG test variables were always the same at the beginning of each part (Table 8). It has only to

be pointed out that at the beginning of each test a crack size measurement was performed in order to update the crack size value that the machine stored in its memory. This allowed to begin approximately at the same point where the previous part was stopped by also introducing the ΔK value at the end of the previous part. To perform the crack size measurement, the software asked for a maximum load to be applied in this measurement, which would be reduced by a factor in % also previously introduced. It was really important that the actual load applied did not exceed the load used in the test, in order to not deform plastically the crack tip.

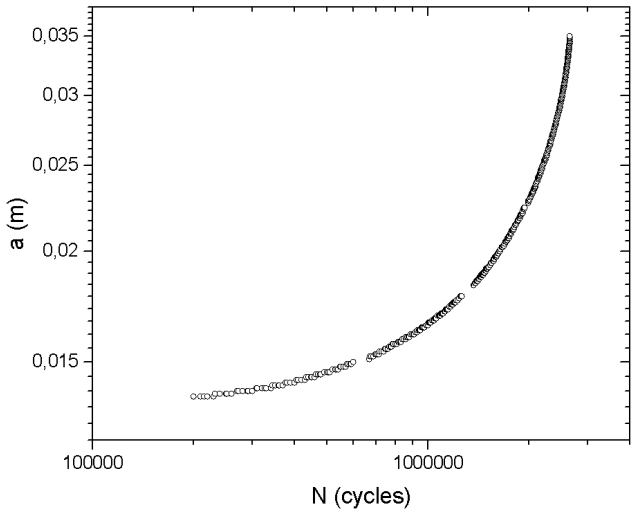

Figure 18. Crack length (a) vs number of cycles (N) for CP0.

Note that part 5 was terminated because the crack size limit was reached at 35 mm. The fatigue crack length grew slower in the first number of cycles, accelerating as N increased (Figure 18). Data of da/dN vs ΔK points provided by the machine in the different parts for CP0 test were used to plot the da/dN vs ΔK curve (Figure 19). It can be seen that the continuity of the curve is quite good, as if it was obtained once in a row. Note that, as already explained; no valid data were obtained for part 0; that is why it is not represented. The curve obtained corresponds mainly to region II in a typical sigmoidal da/dN vs ΔK curve. If the test was continued above $\Delta K > 45$ MPa.m$^{0.5}$ it would be expected that at one point the crack growth rate would increase exponentially until fracture (region III). On the other hand, if the test was continued with $\Delta K < 8$ MPa.m$^{0.5}$ it would be expected that da/dN diminished until reaching ΔK_{th}

(region I).

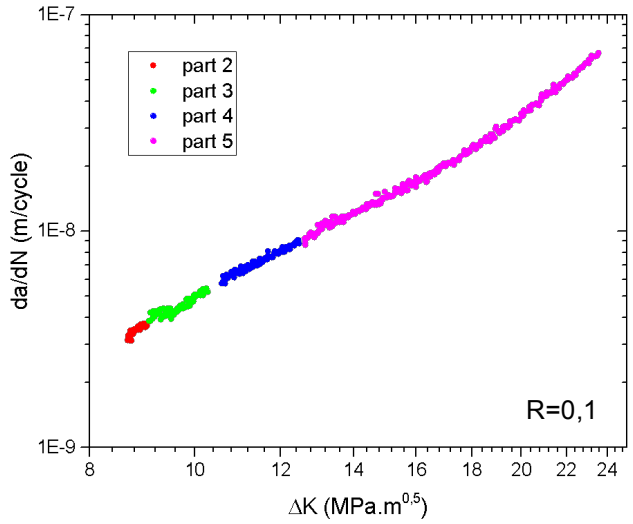

Figure 19. Fatigue crack growth rate (da/dN) vs ΔK for CP0.

8.2. TEST SPECIMEN CP1

FCG for specimen CP1 was performed in one part, all data was recorded all in a row. Figure 20 shows crack length vs number of cycles for this specimen. Again, the crack length doesn't increase much in the first number of cycles, but it accelerates its growth from N = 200.000 cycles.

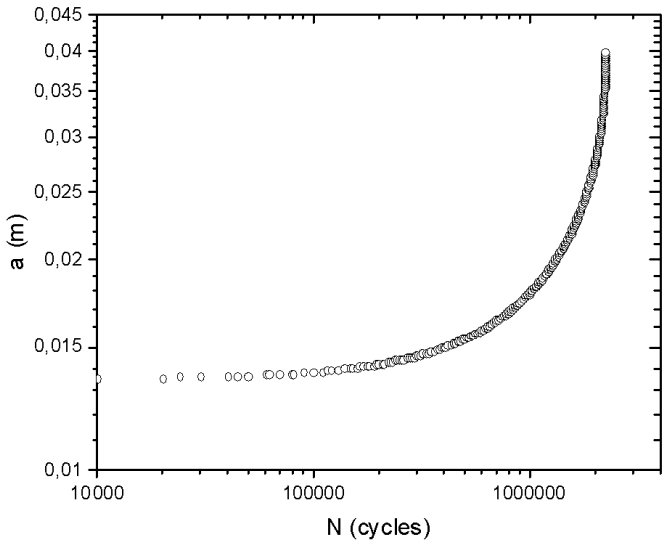

Figure 20. Crack length (a) vs number of cycles (N) for CP1.

The machine stopped since the interlock (upper limit) introduced for the COD was reached at one moment. This happened before the maximum crack size condition was met, at a crack size of 39,8 mm. The interlock value could have been changed (increased) in order to continue with the crack growth, but it would have been under a monotonic load, which is not the interest of this work. Data resulting from CP1 are shown in Table 15:

Table 15. Results after FCG test.

CP1						
PART	Mode	N_f (cycles)	a_f (m)	ΔK (MPa.m$^{0.5}$)	Stop reason	Elapsed time
1	Constant	2,250,528	0.0398	30.627	Interlock	25

The da/dN curve for CP1 is represented in Figure 21. Again, the curve corresponds to region II of a typical da/dN curve. Since all the data was obtained in just one test (just one part), seems that the linearity of the curve its better in this case compared to the curve for CP0. The crack growth rates range from 2 x 10^{-9} to 7 x 10^{-7} m/cycle and ΔK from 8 to 21 MPa.m$^{0.5}$.

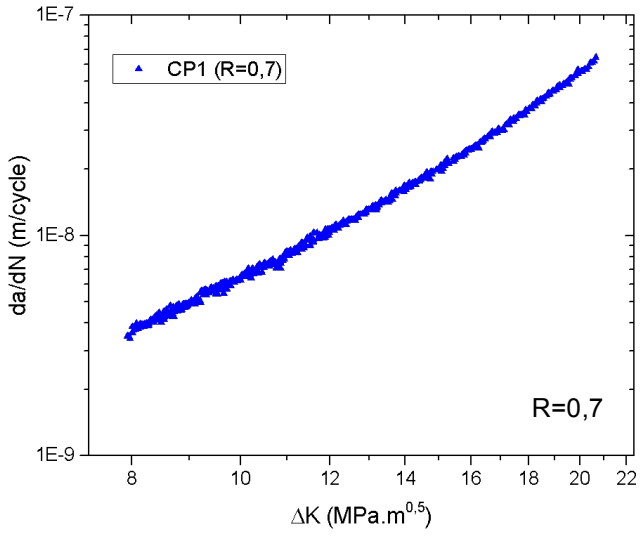

Figure 21. Fatigue crack growth rate (da/dN) vs ΔK for CP1.

8.3. TEST SPECIMEN CP2

Specimen CP2 was tested in four parts using two modes: K-decreasing and constant load. For the K-decreasing mode, it wasn't first thought that so many cycles were going to be needed to find the ΔK_{th}, so the first part was put to end at 3.000.000 cycles. Eventually, more than 15.000.000 of cycles were needed to obtain enough data to provide an acceptable value of ΔK_{th}.

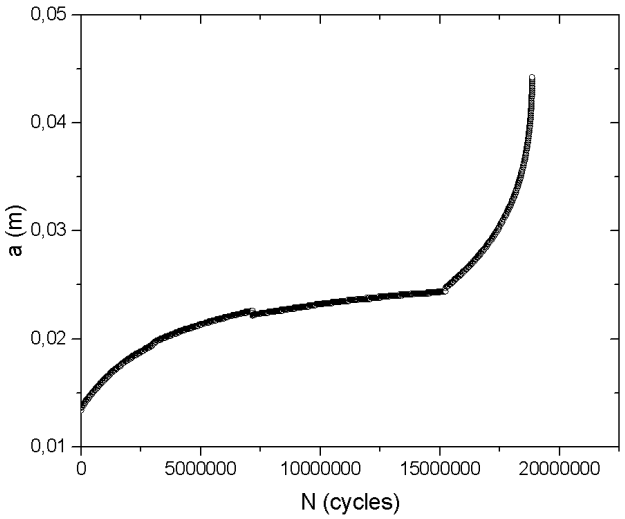

Figure 22. Crack length (a) vs number of cycles (N) for CP2.

Figure 22 shows the evolution of the crack size versus number of cycles. It can be seen that in the first 15.000.000 cycles the crack increases its size but with a lower rate as N increases, defining an asymptote at the end of this first number of cycles. This makes sense since when reaching ΔK_{th}, the crack size would remain constant. Then, the crack size starts growing again with the same behavior seen in CP0 and CP1, corresponding to the constant load mode in part 4.

Data resulting from CP2 are shown in Table 16. Note that from part 1 to part 3, ΔK diminishes at a real slow rate since at the end of part 3 ΔK is really close to ΔK_{th}.

Table 16. Results after FCG test.

CP2						
PART	Mode	N_f (cycles)	a_f (m)	ΔK (MPa.m$^{0.5}$)	Stop reason	Elapsed time
1	K- decreasing	3,000,000	0.019	5.199	Cycles	33.3
2	K- decreasing	4,186,123	0.023	4.049	User	46.5
3	K- decreasing	8,060,000	0.0244	3.264	Machine error	74.6
4	Constant	3,618,995	0.044	22.703	User	40.2

Figure 23 shows the da/dN vs ΔK curve for CP2, were the 4 parts can be distinguished. As in CP0, there is a good continuity between all the parts. As CP2 was tested to obtain ΔK_{th}, the da/dN and ΔK range studied are higher (especially the lower limit) in comparison to the other two specimens.

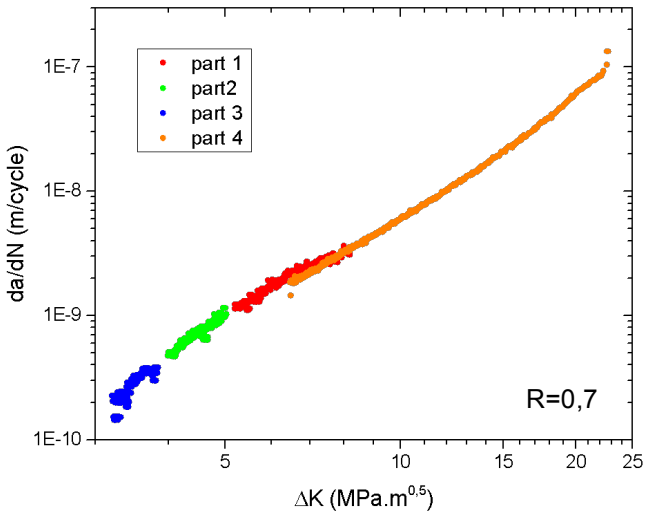

Figure 23. Fatigue crack growth rate(da/dN) vs ΔK for CP2.

When looking to the data obtained by the two different methods, a good continuity can also be established. Figure 24 shows this. The K-decreasing method provided data for da/dN < 10^{-8} m/cycle, as the E647 Standards establishes, and the rest of it by the constant load method. Note that both curves overlap when ΔK is between 6,5 and 8

MPa.m$^{0.5}$, which means that the constant load method was properly started at the same approximate point where the K-decreasing method was started too.

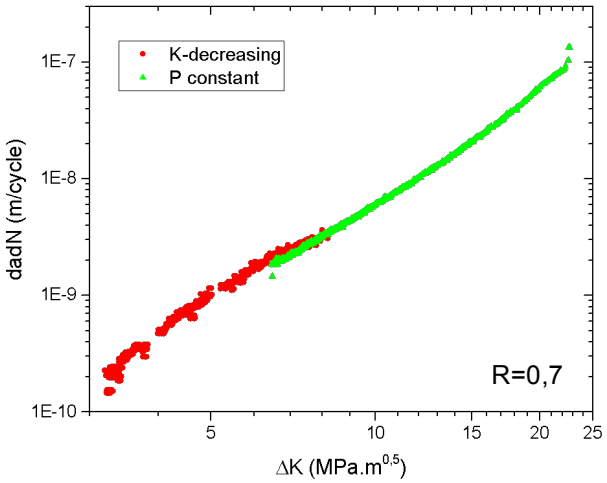

Figure 24. Fatigue crack growth rate (da/dN) vs ΔK for CP2.showing the method used for its testing.

9. ANALYSIS AND DISCUSSION

9.1. CRACK SIZE

Measurements of the precrack and the crack were performed in order to check that the crack size measured by specimen compliance was correct. Specimens were fractured into two pieces revealing the fracture surface and a microscope was used for physical crack length measurements.

For instance, Figure 25 Shows the fracture surface of CP1. The precrack and the crack region can be distinguished very well. The red ash corresponds to the final crack length (the yellow line represents the position of the hole, the initial point from where distances are measured). The length corresponded very well to the ones calculated by the machine (39.8 mm). Hence, the crack length data provided by the machine could be considered correct and used for its treatment and analysis.

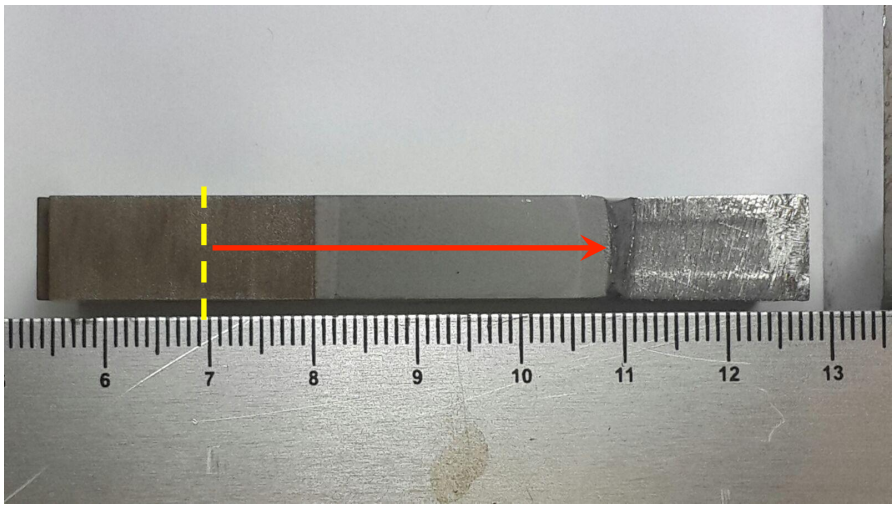

Figure 25. Fracture surface of CP0. Both pre crack and crack surface are easy to distinguish.

9.2. DATA REDUCTION TECHNIQUES

Almost all the data provided by the machine was correct and reliable. In order to check the validity of the machine da/dN vs ΔK data points, the two routines recommended by the E647 Standard were used.

Using MATLAB routines, da/dN vs ΔK curves for the three specimens were plotted using the polynomial (n=4) and secant method. Figure 26, Figure 27 and Figure 28 the results.

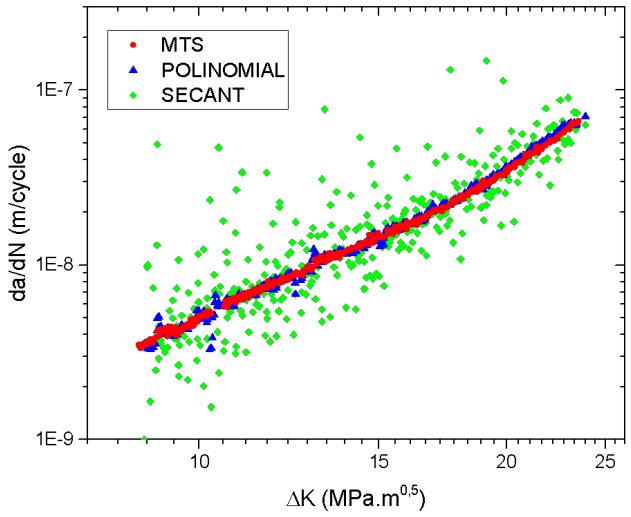

Figure 26. da/dN vs K curves obtained using the machine (MTS), the incremental polynomial method (POLYNOMIAL) and the secant method (SECANT) for CP0.

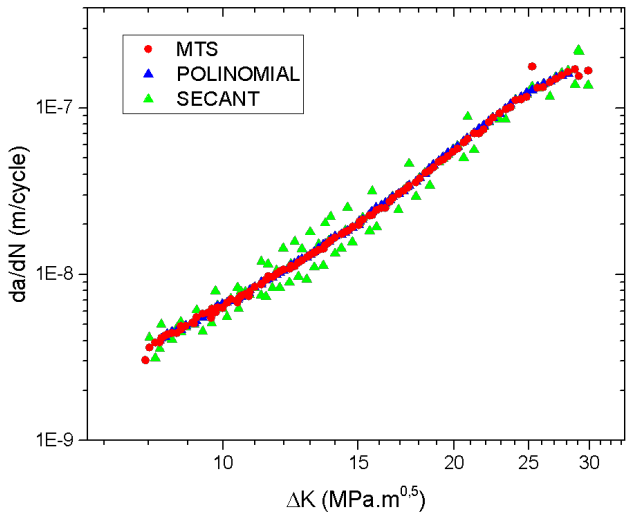

Figure 27. da/dN vs K curves obtained using the machine (MTS), the incremental polynomial method (POLYNOMIAL) and the secant method (SECANT) for CP1.

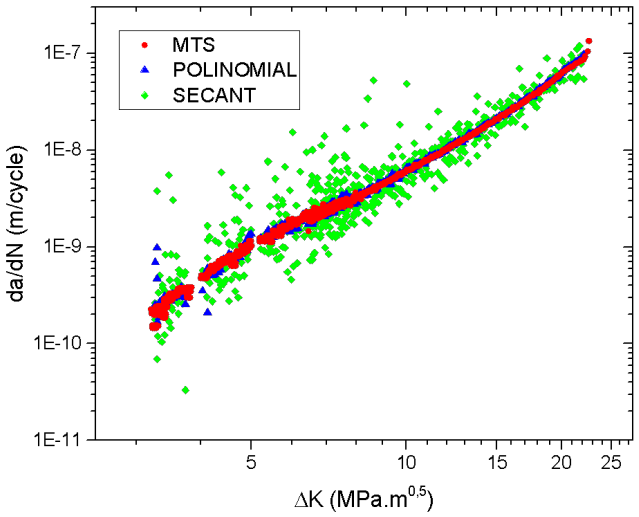

Figure 28. da/dN vs K curves obtained using the machine (MTS), the incremental polynomial method (POLYNOMIAL) and the secant method (SECANT) for CP2.

It can be seen that for all cases, the secant method doesn't provide good results for in these cases. Especially for CP0 and CP2, the points are very dispersed and far away from those provided by the machine (noted as MTS). Note that even in some cases, even not plotted here, secant method provided negative da/dN values, which makes completely no sense at all (it would mean that, somehow, the crack is closing itself reducing its crack size instead of growing).

On the other hand, the polynomial method fits very well the machine values in all cases. Just for CP2, at low da/dN and ΔK values when using K-decreasing method, polynomial points seem to disperse a bit.

This difference between both methods is, in fact, pointed out in E647 Standard, standing that the secant method often results in increased scatter in da/dN relative to the incremental polynomial method since the second one smooths the data numerically.

In this line, if the machine did not provide the da/dN curves, the incremental polynomial method would be the best method to obtain the curves in these cases, since they match pretty well the machine curves.

9.3. FATIGUE CRACK GROWTH RATE VS STRESS INTENSITY FACTOR CURVES (da/dN vs ΔK)

In total, three da/dN vs ΔK curves for API X65 steel showed in Figure 29. For CP0 and CP1, fatigue crack growth rates were obtained in a range from 2 x 10^{-9} to 7 x 10^{-8} m/cycle, approximately. For CP2, the range obtained is 1 x 10^{-10} to 1 x 10^{-7}m/cycle approximately, since a wider range of ΔK was tested in this case in comparison to the other two specimens.

CP0 and CP1 curves correspond to region II in a typical da/dN vs ΔK curve. In CP2, both regions I and region II were obtained.

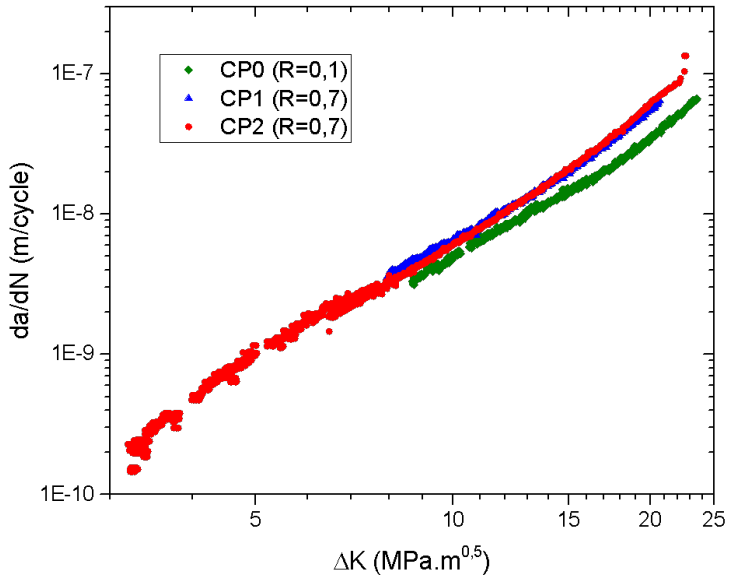

Figure 29. da/ dN vs ΔK curves for the three specimens tested.

Kim et al. obtained da/dN vs ΔK curves for three API steels, X65, X70 and X80 in TL orientation, the same studied for CP0, CP1 and CP2 (Kim, 2011). Their results for X65 are similar to the ones obtained in this work (Figure 30). Although the test conditions not exactly the same (frequency of 20Hz and R=0.1 for all specimens) a comparison of the crack growth rates can be established.

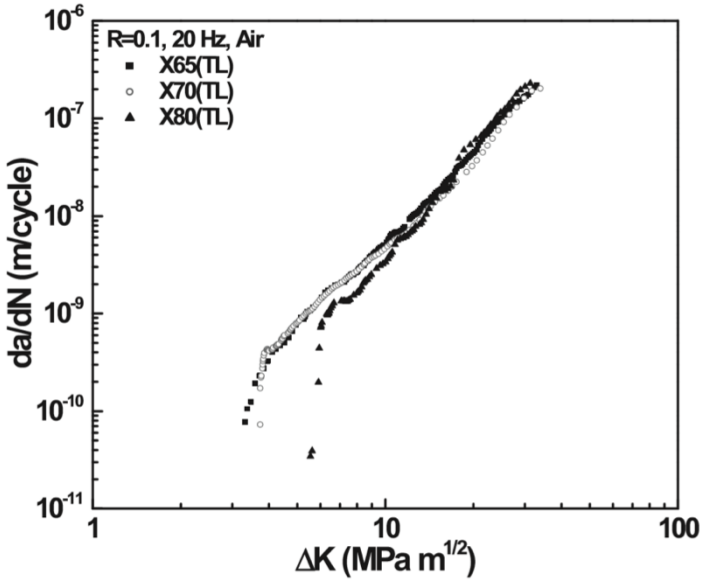

Figure 30. da/dN vs ΔK curves for API X65, X70 and X80 at R=0.1 (Kim, 2011).

Focusing in CP0, which was tested at the same R (CP1 and CP2 are ignored now, since the effect of R will be discussed later), region II seems to be quite the same in both cases as well as the da/dN values. For instance, in this work was found that for a ΔK = 10 MPa.m$^{0.5}$ the da/dN value expected is 4 x10^{-9}m/cycle for CP0. The value of da/dN at the same ΔK in Kim et al. study is almost exactly the same.

Table 17. Comparison of data points obtained for X65 in this work and other authors. (*) Extrapolated value.

ΔK (MPa.m$^{0.5}$)	da/dN (m/cycle)	
	This work	Kim et al.
8	1.5 x 10^{-9} (*)	1 x 10^{-9}
10	5 x 10^{-9}	5 x 10^{-9}
20	3.5 x 10^{-8}	4 x 10^{-8}

From results in Table 17, it could be said that curves obtained is both works are almost the same. Since region I was not obtained for CP0, this will allow to use Kim et al. curve to discuss a value of ΔK_{th} for X65 at R=0.1 since they did obtain region I and II

in their work. This will be done later on, when discussing ΔK_{th} values.

9.4. PARIS LAW

Region II of the three specimens were obtained and used to calculate the Paris Law for each one. To this end, log (da/dN) vs log(ΔK) curves were plot, as shown in Figure 31. As should be, the three curves are quite linear. At first glance, CP1 and CP2, tested at the same R, overlap pretty well. This makes sense since it would be expected to obtain a similar da/dN vs ΔK curve for both specimens.

For a fixed value of ΔK, da/dN values for CP0 are lower to the ones in CP1 and CP2. This is because of the different R. As already discussed, when increasing R the curve remains its shape but it translates to the left.

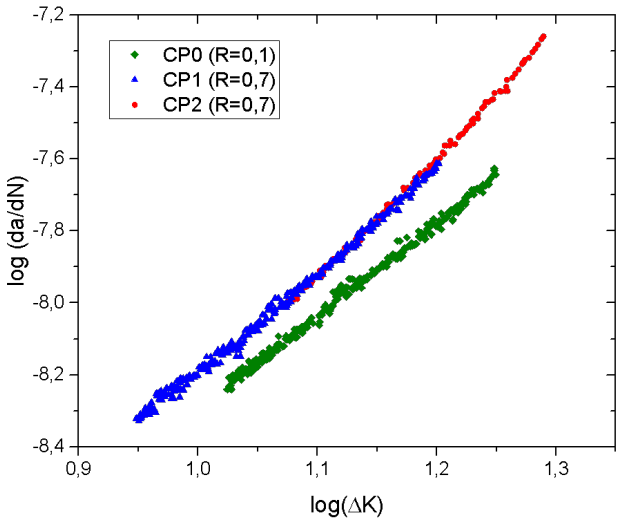

Figure 31. log (da/dN) vs log(ΔK) curves for the three specimens tested showing region II.

Figure 32 shows the linear fit for each specimen, from which the Paris Law constants were extracted. CP0 and CP1 slopes are pretty parallel. These values are shown in Table 18. Note that these constants are calculated for da/dN given in m/cycle and ΔK in $MPa.m^{0.5}$.

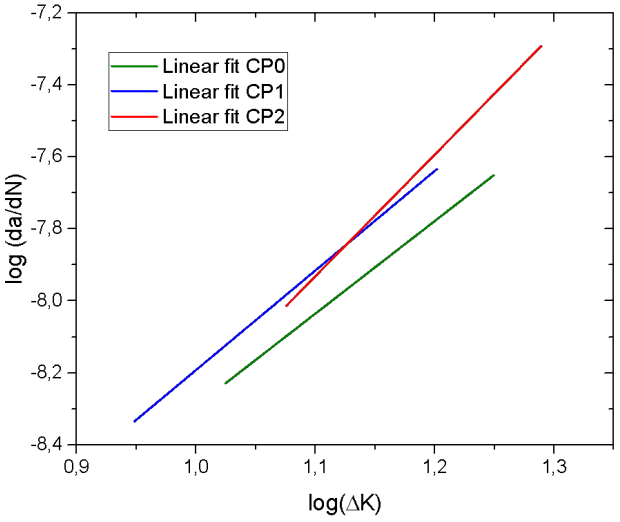

Figure 32. Region II linear fits for CP0, CP1 and CP2.

Table 18. Paris law constants values for the three specimens tested.

Specimen	R	m	C
CP0	0.1	2.57	1.37×10^{-11}
CP1	0.7	2.76	1.10×10^{-11}
CP2	0.7	3.37	2.25×10^{-12}

Slope (*m*) values confirm the parallelism between CP0 and CP1. Although it would be expected that CP1 and CP2 shared the same slope, this is not the case, there is a mismatch. The slope value is sensitive to the data chosen for its calculation, so little differences in machine data values between data from CP1 and CP2 translate in different resulting m values. Hence, this mismatch in the expected values for m might be due to experimental randomness.

These results were confronted to results for API steels of other authors in Table 19.

Table 19. Paris law constant values of some API steels.

Author	Material	R	m	C
(Fernandes,	X60	0.1	3.61	5.13×10^{-10}
(Fernandes,	X60	0.7	4.74	4.35×10^{-9}
(Vosikovski,	X65	0.05	3.53	1.33×10^{-9}
(Beltrao, 2010)	X70	0.1	4.59	2.06×10^{-11}
(Beltrao, 2010)	X70	0.5	3.28	3.73×10^{-9}
(Briottet, 2011)	X80	0.1	3.1	2.5×10^{-9}

The values obtained in this work are in the range of the results of other studies. Remembering that m expected values for metallic materials range from 2 to 5, the ones obtained here seem correct.

9.5. EFFECT OF R

Since two load ratios were used for the tests its influence can be studied. It is known that R has a direct impact in fatigue threshold values that is discussed later. Figure 33 shows the da/dN curves for CP0 (R=0.1) and CP1 (R=0.7). Both curves are almost the same; one seems the copy of the other one but translated. It is expected that this translation is even bigger in regions I and III of the curve, which are very sensitive to changes in R.

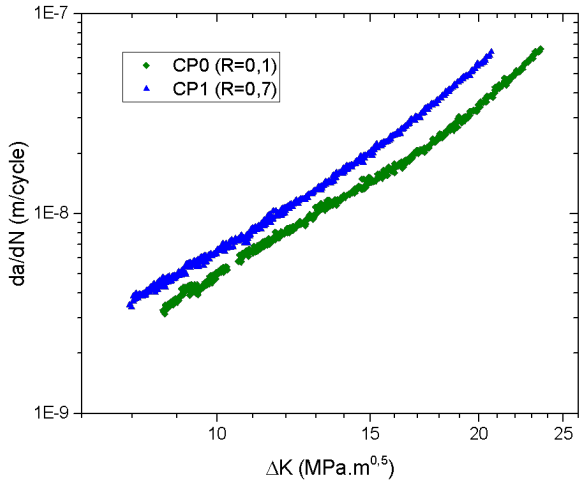

Figure 33. da/dN vs ΔK curves of CP0 and CP1.

Paris Law coefficient "m" for CP0 and CP2 is very similar between them, meaning that the slopes are pretty similar and that both could be the same curve, but they are just separated by a translation movement. Since C coefficient is the y-axis intercept value, a difference in its value is expected when changing R. Given a da/dN curve at certain R, for higher values of R the curve translates to the left and to the right for lower ones.

9.6. THRESHOLD VALUES

A threshold fatigue crack value was obtained for CP2. Using the last 5 data points where 10^{-10} < da/dN < 10^{-9} m/cycle, a linear fit was calculated and the ΔK_{th} obtained was that value of ΔK which corresponded to a fatigue crack growth rate of 10^{-10} m/cycle (Figure 34). Such value is ΔK_{th} = 3.17 MPa.$m^{0.5}$ for CP2.

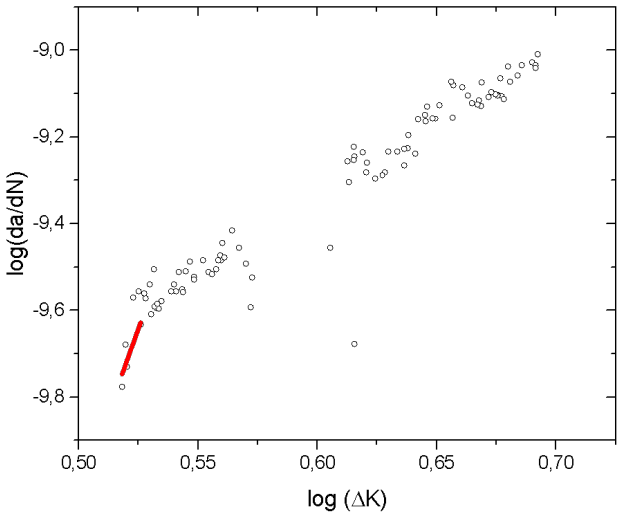

Figure 34. Linear fit of the 5 points showing the lowest values of da/dN used for computing ΔK_{th}.

A similar value is obtained when, in a ruder way, ΔK_{th} is calculated as the mean average of the 10 points showing the lowest value of ΔK. The value obtained like so is $\Delta K_{th'} = 3{,}23$ MPa.m^{0,5}.

As seen before, when analyzing the da/dN vs ΔK curves, the one found in this work for CP0 and the one obtained by Kim et al. for X65 at R=0.1 are pretty identical. Since region I is missing in this work for CP0, the assumption that region I for CP0 and the one in Kim et al. work are the same can be reasonably accepted. The ΔK_{th} value found in their work for X65 at R=0.1 was 3.32 MPa.m$^{0.5}$, so this is that one assumed to be equal for CP0.

Then, when establishing a comparison between ΔK_{th} values for X65 CP0 (R=0.1) and CP2 (R=0.7), it is found that, indeed, the value for CP2 is lower than the one for CP0. As already explained, when increasing R, ΔK_{th} decreases. The difference, however, is not big. To establish a better comparison, a more accurate value for CP2 should be found, which could be done achieving lower growth rates values, below 1 x 10^{-11} m/cycle.

To explain this difference in ΔK_{th} values, the crack closure phenomenon is usually cited. The crack closure is more probable to occur at low R than at high ones, since for

the last caseloads are very high and the crack is opened for all the range of load applied.

Hence, crack closure could be pointed out to try to explain the difference of ΔK_{th} values for X65 at R=0.1 and R=0.7. However, in this particular case, it is already known that there is no crack closure for X65 at R=0.1 from Kim et al. results in their study. Presumably, for CP2 there is no crack phenomenon neither since it was tested at R=0.7. Fatigue threshold values for API steels are not very frequent in the literature, especially for high R. Table 20 shows some ΔK_{th} values for different API steels at R=0.1 and R=0.7.

Table 20. Fatigue threshold values of some API steels at different R.

Author	Material	R	ΔK_{th} (MPa.m$^{0.5}$)
(Kim. 2011)	X65	0.1	3.32
(Kim. 2011)	X70	0.1	3.74
(Kim. 2011)	X80	0.1	5.62
(Kwon. 2006)	X80	0.7	5.92

The value found for CP2 is in the range of the values for API steels, so could be considered correct. Note that the threshold value is higher for higher grades of API steels. This makes sense since higher-grade API steels, such as X80, are tougher and more mechanically resistant than, for instance, X65.

10. CONCLUSIONS

- The crack size measured by the specimen compliance is accurate, as shown physically for the precrack and final crack lengths.
- The shape of da/dN vs ΔK curves plotted for all three specimens are consistent with the theory and the range of experimental C and m values is coherent with literature values.
- Performing a FCG test in parts, although preferably performed without the test machine stopping, provided continuous and correct data when starting the parts with the right FCG test parameters values, as shown for CP0 and CP2.
- Using one specimen, both da/dN vs ΔK curve and fatigue threshold value can be obtained using first the K-decreasing method followed by the constant load method, as done for CP2.
- The incremental polynomial method provided the closest results to the test machine, in comparison to the secant method. If the machine did not provide the da/dN curves, the polynomial method would then be the best one to obtain them.
- The effect of R was evaluated in CP0 and CP1, showing that the working at higher load ratios translated the curve to the left, as expected.
- The threshold value found for CP2 at R=0,7 (ΔK_{th} = 3,17 MPa.m$^{0.5}$) is coherent with the literature.

At the end of this work, some suggestions are done for future works:

- More fatigue threshold values should be obtained in order to be able to make a solid comparison between specimens. This could be obtained at different load ratios to evaluate its influence.
- Establish a comparison with other API steels, such as X65, X70 and X80.
- Evaluating the fatigue properties in other critical zones of welded pipelines, such as

the welded zone and thermally affected zone (ZTA) for X65 and other API steels at R=0.7.

- Compare these results with others in other environments, such as seawater.

REFERENCES

Anglada, M. (2002). Fractura de materiales. *Edicions UPC*.

API 5L Standard. (2004). Specification for Line Pipe (Amercian Petroleum Institue).

Beltrao, M. N. (2010). Fatigue crack propagation in API 5L X-70 pipeline steel longitudinal welded joints under constant and variable amplitudes. *Fatigue and Fracture Engineering Materials and Structures*.

Briottet, I. (2011). Quantifying the hidrogen embrittlement of pipe steels for safety consideration.

Clennel, R. (2004). *Subsea Pipeline Engineering.* PennWell Books.

Corbett, K. (1988). High Strength Steel Pipeline Economics. . *Proceedings of The Thirteenth International Offshore and Polar Engineering Conference.*

Dowling, N. (2007). *Mechanical behavior of materials.* Nova Jersey: Pearon-Prentice Hall.

E647 ASTM Standard. (2011). *Standar test method for measurement of fatigue crack grwoth rates,.*

Fernandes, J. (2002). *Uma metodologia para a analise e modelagem de tensoes residuais.* Rio de Janeiro : PhD thesis, PUC.

Fracturemechanics.org. (s.d.).

Herynk, M. (2007). Effects of the UOE/UOC pipe manufacturing processes on pipe collapse pressure. . *Int. J. Mech. Sci.* , 533-553.

Hillenbrand, H. (1997). Considerations for Welding X80 Line Pipe Established. . *Oil & Gas Journal. , 37*.

Kim, Y. (2011). Near threshold fatigue crack growth behavior and crack closure of natural gas pipeline steels. . *Procedia Engineering*, 813-820.

Kujawski, F. (1987). A fatigue crack growth model with load ratio effects. . *Eng. Fracture Mechanics*, 337-367.

Kwon, D. (2006). Fatigue Behavoir of API-80 Steels. . *ICONE 14*.

Malcoln, J. (2007). A Guide for Understanding & Specifying Chemical Composition of High Strength Linepipe Steels. . *Companhia Brasileira de Metalurgia e Mineração.*

Marcus, A. H. (1999). On crack closure and crack tip shielding during fatigue crack growth. . *Review of Progress in Qualitative Nondestructive Evaluation, , 18*.

N.T. Board. (2004). Anhydrous ammonia pipeline rupture.

Ordoñez, R. (2004). Soldagem E Caracterização das Propriedades Mecânicas de Dutos de Aço API 5L X80 Com Diferentes Arames Tubulares. . *Dissertaçao (Mestrado). Universidade Estadual de Campinas.*

Ritchie, R. (1977). Influence of microstructure on near-threshold fatigue crack propagation in ultra-high strength steel. . *Metal Science 11*, 368-381.

SANTOS, P. F. Estudo de Técnicas de Tratamento de Dados Experimentais para a Avaliação da Curva da/dN versus Delta-K – Um Estudo para o Aço ASTM A743 CA6NM. Dissertação de Mestrado em Integridade de Materiais de Engenharia. Publicação FGA.DM - 001A/2013, Programa de Pós-Graduação em Integridade de Materiais da Engenharia, Universidade de Brasília – Faculdade do Gama/Faculdade de Tecnologia, Brasília, DF, 254p

Soeiro, J. (2013). Uma breve revisão histórica do desenvolvimento da soldagem dos aços API para tubulações. . *Sodag. insp., 18*.

Totten, G. (2008). Fatigue crack propagation. *Advanced Materials and Processes*.

Velázquez, J. (2004). Mecánica de la fractura. *Limusa*.

Vosikovski, O. (1981). Growth of surface fatigue cracks in a steel plate. . *Int. J. Fatigue 3*, 11-115.

Zehnder, A. (2010). Fracture Mechanics. *Universidad de Cornell*.

ANNEXES

ANNEXE I: MATLAB CODE

SECANT METHOD

```
close all
clear all

tab=xlsread(Excel_file_name.xls');
format long e

N=tab(:,1);
a=tab(:,2);
Kmax=tab(:,3);
Kmin=tab(:,4);
Fmax=tab(:,5);
Fmin=tab(:,6);
Dv=tab(:,7);

%all in SI units
W=0.060;
B=0.010;

%Constants for crack size calculus obtained from E647

c0=1.0010;
c1=-4.6695;
c2=18.460;
c3=-236.82;
c4=1214.9;
c5=-2143.6;
```

```
%material features

yield=547000000;
E=210000000000;

DK=Kmax_m(:,:)-Kmin(:,:);
DF=Fmax_m(:,:)-Fmin(:,:);

i=size(DK,1);

k=1;
t=2;

for k=1:i

   compliance(k,1)=E*Dv(k,1)*B/DF(k,1);
   ux(k,1)=((sqrt(compliance(k,1))+1))^(-1);

   a_comp(k,1)=W*(c0+c1*ux(k,1)+c2*ux(k,1)^2+c3*ux(k,1)^3+c4*ux(k,1)^4+c5*ux(k,1)^5);

   k=k+1;
end

for t=2:i

   da(t,:)=a(t,1)-a(t-1,1);
   dN(t,:)=N(t,1)-N(t-1,1);

   dadN(t,:)=da(t,1)/dN(t,1);

   at(t,:)=a(t,1)+a(t-1,1)/2;
   Nt(t,:)=N(t,1)-N(t-1,1)/2;

   alfa(t,:)=at(t,:)/W;
```

```
   DK_comp(t,:)=DF(t,:)*(10^(-3/2))/(B*sqrt(W))*(2+alfa(t,:))/((1-
alfa(t,:))^1.5)*(0.886+4.64*alfa(t,:)- 13.32*alfa(t,:)^2+14.72*alfa(t,:)^3-5.6*alfa(t,:)^4);
```

POLYNOMIAL METHOD

```
close all
clear all

format short e;

tab=xlsread('Excel_file_name.xls')

N=tab(:,1);
a=tab(:,2);
Kmax=tab(:,3);
Kmin=tab(:,4);
Fmax=tab(:,5);
Fmin=tab(:,6);

W=0.06
B=0.01

DK=Kmax(:,:)-Kmin(:,:);
DF=Fmax(:,:)-Fmin(:,:);

i=size(DK,1);
n=4;
k=n+1;

for k=n+1:i-n
   N1=N(k-n:k+n,1);
   a1=a(k-n:k+n,1);
   C1=(N1(1,1)+N1(end,1))/2;
   C2=(N1(end,1)-N1(1,1))/2;
```

```
    x(:,:)=(N1(:,:)-C1)/C2;

    y=polyfit(x,a1,2);
    b2=y(:,1);
    b1=y(:,2);
    b0=y(:,3);

    a_poly(k,1)=b0+(b1*(N1(n+1,1)-C1)/C2)+(b2*(((N1(n+1,1)-C1)/C2)^2));
    dadN_poly(k,:)=(b1/C2)+2*b2*(N1(n+1,1)-C1)/(C2^2);

    alfa(k,:)=a_poly(k,:)/W;

    DK_poly(k,:)=(DF(k,:)/(B*sqrt(W)))*((2+alfa(k,:))/((1- alfa(k,:))^(3/2)))*(0.886+4.64*alfa(k,:)-
13.32*alfa(k,:)^2+14.72*alfa(k,:)^3-5.6*alfa(k,:)^4);

    k=k+1;

end
```